blood RCI
red cells & iron

American Society of Hematology
2021 L Street NW, Suite 900,
Washington, DC 20036
Phone: 202-776-0544 | Fax 202-776-0545
bloodrci@hematology.org

Red cell shape regulation by band 3–ankyrin–spectrin linkage: Implications for clinical severity of bovine HS

Tracking no: RCI-2025-000113R1

Kosuke Miyazono (Hokkaido University, Japan) Mizuki Tomihari (Hokkaido University, Japan) Nobuto Arashiki (Tokyo Women's Medical University, Japan) Ichiro Koshino (Tokyo Women's Medical University, Japan) Yayoi Otsuka-Yamasaki (Hokkaido University, Japan) Kota Kizaki (Hokkaido University, Japan) Takashi Tsukamoto (Hokkaido University, Japan) Osamu Inanami (Hokkaido University, Japan) Ayumi Deguchi (Hokkaido University, Japan) Eri Kitaguchi (Jichi Medical University, Japan) Makoto Demura (Hokkaido University, Japan) Narla Mohandas (New York Blood Center, United States) Yuichi Takakuwa (Tokyo Women's Medical University, Japan) Mutsumi Inaba (Hokkaido University, Japan)

Abstract:
The mechanical stability and shear elasticity of the red cell membrane are regulated by the proteins of the membrane skeleton consisting of rod-like α2β2 spectrin tetramers attached at their distal ends to the junctional complexes, while the stability of the lipid bilayer is maintained by the linkage between transmembrane proteins, such as band 3, and the underlying spectrin-based skeleton. While it has long been suggested that the lipid bilayer–membrane skeleton linkage is also involved in stabilizing the spectrin-based skeleton, no naturally occurring cases exist to substantiate this hypothesis. Here we report that a novel substitution mutation in bovine α-spectrin E91K, located in the middle of the first spectrin repeat α1, causes disruption of the stable triple-helical bundle of this domain and impairs the spectrin dimer–dimer self-association, resulting in decreased spectrin tetramer formation leading to pronounced decrease in red cell mechanical stability. The E91K substitution markedly exacerbated the loss of membrane surface areas in hereditary spherocytosis (HS) due to band 3 deficiency, presumably through the increased membrane fragmentation. Notably, the red cells carrying E91K substitution and normal band 3 contents showed only mild spectrin deficiency without significant hematologic abnormalities, while upon perturbation of band 3–ankyrin association exhibited disruption and fragmentation of the spectrin network. Taken together, these findings demonstrate that the band 3–ankyrin–spectrin linkage plays a key role in promoting and reforming of the spectrin tetramer to maintain mechanical stability and deformability of the membrane skeleton, in addition to stabilizing the lipid bilayer in red cells.

Conflict of interest: No COI declared

COI notes:

Preprint server: No;

Author contributions and disclosures: M. I. designed the research; K. M., M. T., T. T., O. I., and M. I. designed experiments, performed experiments, and analyzed the data; N. A., I. K., and Y. O.-Y. performed experiments and analyzed the data; M. D. analyzed the data; K. K., A. K., and E. K. performed experiments; K. M., M. T., and M. I. wrote the original manuscript; N. M., Y. T., and M. I. analyzed the data, made critical intellectual contributions throughout the research, and edited the manuscript.

Non-author contributions and disclosures: No;

Agreement to Share Publication-Related Data and Data Sharing Statement: For original data, please contact the corresponding author, Mutsumi Inaba (inazo@vetmed.hokudai.ac.jp). DNA sequences of bovine SPTA1 and SPTB were deposited in GenBankTM with accession numbers OL303989 (SpαA), OL303990 (SpαB), OL303991 (SpαBK91), OL303992 (SpβA), and OL303993 (SpβB), respectively.

Clinical trial registration information (if any):

Regular Article

Red cell shape regulation by band 3–ankyrin–spectrin linkage: Implications for clinical severity of bovine HS

●Running head title: Band 3 function in spectrin tetramer formation

Kosuke Miyazono,[1] Mizuki Tomihari,[1, 2] Nobuto Arashiki,[1, 3] Ichiro Koshino,[2, 3] Yayoi Otsuka-Yamasaki,[1] Kota Kizaki,[1] Takashi Tsukamoto,[4] Osamu Inanami,[5] Ayumi Deguchi,[1] Eri Kitaguchi,[1] Makoto Demura,[4] Narla Mohandas,[6] Yuichi Takakuwa,[3] and Mutsumi Inaba[1, 2,]

[1]Laboratory of Molecular Medicine, Graduate School of Veterinary Medicine, Hokkaido University, Sapporo 060-0818, Japan; [2]Laboratory of Clinical Pathobiology, Graduate School of Agricultural and Life Sciences, University of Tokyo, Tokyo 113-8657, Japan; [3]Department of Biochemistry, School of Medicine, Tokyo Women's Medical University, Tokyo 162-8666, Japan; [4]Laboratory of Biological Information Analysis Science, Faculty of Advanced Life Science, Hokkaido University, Sapporo 060-0810 Japan; [5]Laboratory of Radiation Biology, Graduate School of Veterinary Medicine, Hokkaido University, Sapporo 060-0818, Japan; and [6]Red Cell Physiology Laboratory, New York Blood Center, New York, NY 10065

●Correspondence author: Mutsumi Inaba, Laboratory of Molecular Medicine, Faculty of Veterinary Medicine, Hokkaido University, Sapporo 060-0818, Japan; email: inazo@vetmed.hokudai.ac.jp; Phone: +81-11-706-5580; Fax: +81-11-706-5276

●Text word count: 3,997 words
●Abstract word count: 250 words
●Figure/Table count: 5 Figures and 1 Table
●Reference count: 50

Key Points

●Band 3–ankyrin–spectrin link promotes spectrin tetramerization to maintain mechanical stability and deformability of the red cell membrane.

●The E91K substitution in α-spectrin destabilizes spectrin tetramerization and exacerbates spherocytic phenotype due to band 3 deficiency.

Abstract

The mechanical stability and shear elasticity of the red cell membrane are regulated by the proteins of the membrane skeleton consisting of rod-like $\alpha_2\beta_2$ spectrin tetramers attached at their distal ends to the junctional complexes, while the stability of the lipid bilayer is maintained by the linkage between transmembrane proteins, such as band 3, and the underlying spectrin-based skeleton. While it has long been suggested that the lipid bilayer–membrane skeleton linkage is also involved in stabilizing the spectrin-based skeleton, no naturally occurring cases exist to substantiate this hypothesis. Here we report that a novel substitution mutation in bovine α-spectrin E91K, located in the middle of the first spectrin repeat α1, causes disruption of the stable triple-helical bundle of this domain and impairs the spectrin dimer–dimer self-association, resulting in decreased spectrin tetramer formation leading to pronounced decrease in red cell mechanical stability. The E91K substitution markedly exacerbated the loss of membrane surface areas in hereditary spherocytosis (HS) due to band 3 deficiency, presumably through the increased membrane fragmentation. Notably, the red cells carrying E91K substitution and normal band 3 contents showed only mild spectrin deficiency without significant hematologic abnormalities, while upon perturbation of band 3–ankyrin association exhibited disruption and fragmentation of the spectrin network. Taken together, these findings demonstrate that the band 3–ankyrin–spectrin linkage plays a key role in promoting and reforming of the spectrin tetramer to maintain mechanical stability and deformability of the membrane skeleton, in addition to stabilizing the lipid bilayer in red cells.

Introduction

To survive in the circulation while being subjected to continuous shear stress conditions for over 100 days, the red blood cell (RBC) must be highly flexible and durable, undergoing marked reversible deformation without fragmentation or the loss of membrane surface area. The RBC deformability and stability are maintained by the structural organization of membrane skeletal proteins, transmembrane proteins, and the lipid bilayer.

The membrane skeleton supports the structural integrity of human RBCs by providing the mechanical stability against shear deformation.[1–4] Spectrin, actin, and protein 4.1R are the principal components of the membrane skeletal network. Spectrin is a long, flexible rod-like protein consisting of multiple spectrin repeats. Spectrin α and β chains associate with each other to form the αβ heterodimer in an antiparallel fashion and spectrin tetramers are formed by head-to-head self-association of two dimers. Distal ends of spectrin dimers are connected to short F-actin filaments and 4.1R within the junctional complex.[4–6] The spectrin skeletal network is linked to the lipid bilayer through interactions with transmembrane proteins, specifically spectrin–ankyrin–band 3 and spectrin–4.1R–glycophorin C associations.[7–9] Such vertical interactions allow the membrane skeleton network to stabilize the membrane lipid bilayer.[4, 10–13] Various mammalian red cell membranes appear to share these principal structural and functional organization.[14–20]

Defects in these interactions lead to membrane fragmentation or surface area loss associated with abnormal shape changes such as hereditary elliptocytosis (HE) and hereditary spherocytosis (HS) and resulting hemolytic anemias. The principal lesion of HE involves horizontal interactions, primarily spectrin tetramer formation due to mutations at the NH_2-terminus of α-spectrin or the COOH-terminus of β-spectrin.[12, 21, 22] On the other hand, a weakening of the vertical interaction is a common feature of HS. The lipid bilayer with reduced support by the membrane skeleton is destabilized, leading to release of skeleton-free vesicles and resultant spherocytosis.[13]

We previously showed that the total deficiency of band 3 due to a premature termination mutation in *SLC4A1* in bovine RBCs led to loss of band 3–ankyrin–spectrin linkage, thereby markedly reducing the cohesion between the lipid bilayer and the spectrin-based skeleton resulting in severe spherocytosis.[14] However, the RBC membrane pathology differed significantly in one respect from that of the band 3-null mouse models.[15, 16] The spectrin content of bovine band 3-deficient RBCs was reduced by approximately 50%, and vesicle fragments from these RBCs contained spectrin, suggesting that bovine band 3 deficiency is implicated in not only reducing the membrane surface area but also in the lateral interactions of the membrane skeletal proteins. In contrast, the spectrin content and the structure of the membrane

skeleton in band 3-deficient murine RBCs and band 3-null human RBCs were nearly normal.[15, 16, 23, 24]

In this regard, an earlier study[25] suggested that spectrin–ankyrin interaction of high affinity ($K_a = 10^{-7}$ M) constrains the spectrin to a narrow sub-membranous space resulting in high local concentration of spectrin (> 10^{-4} M) enabling effective tetramer formation. Furthermore, the interactions between spectrin, ankyrin, and band 3 *in vitro* were coupled in a positively cooperative manner.[26] Moreover, disruption of the band 3–ankyrin–spectrin link led to dissociation of a large proportion of the spectrin tetramers into dimers.[27] Collectively, these findings have suggested that the band 3–ankyrin–spectrin linkage contributes not only to the lipid bilayer stabilization but also to the formation of spectrin tetramers. However, to date there have been no clinical cases or biological models to clearly demonstrate this hypothesis *in vivo*.

In the present study, we report that a novel substitution E91K in α-spectrin, found in several cases of bovine band 3 deficiency induces structural disruption of the spectrin repeat α1 leading to destabilization of the spectrin tetramer. While the E91K substitution exacerbates the primary phenotype of band 3 deficiency, it causes only mild spectrin reduction and no significant abnormalities in RBCs with normal band 3 content. These findings provide substantial *in vivo* evidence to support a pivotal role for band 3–ankyrin–spectrin linkage in promoting the mechanical properties of RBC membrane skeleton.

Methods

Animals

Band 3-deficient Japanese black cattle homozygous for the R664X mutation of *SLC4A1*[14] and healthy control Japanese black cattle were kept at the animal experimentation facility of the Veterinary School of Hokkaido University. All experimental procedures were approved by the Laboratory Animal Experimentation Committee, Graduate School of Veterinary Medicine, Hokkaido University with an approval number 18040. All other cattle were housed at several different locations in Japan, and their blood samples anticoagulated with EDTA were transported to Hokkaido University for analysis.

Clinical studies

Routine hematological parameters were determined using the hematological analyzer ProCyte (IDEXX Laboratories). Microscopic examination of red cells and reticulocytes was carried out as described previously.[14]

Morphological analyses of RBCs

Scanning electron micrography was performed as described previously.[14] RBC vesiculation/fragmentation was examined under phase-contrast light microscopy after incubation of washed RBCs in phosphate-buffered saline (PBS, 10 mM sodium phosphate (NaPi), pH 7.4, 154 mM NaCl) and also at ambient temperature for 6 hours. RBCs bearing extruded vesicles were counted for 200 RBCs.

Analyses of RBC membrane proteins

Preparation of RBC membrane ghosts and Triton X-100-extracted membrane skeletons (Triton shell), SDS-PAGE, and immunoblotting to analyze membrane proteins including band 3, spectrin, 4.1R, and ankyrin were performed as described previously.[14, 17, 18, 20, 18, 29] The abundance of different polypeptides was determined by densitometric scanning of SDS-gels stained with Coomassie brilliant blue using the ChemDoc imager (Bio-Rad) and the Image Lab software (Bio-Rad). Detection and imaging of immunoblots were similarly performed.

Induction of vesicle formation from RBCs

RBCs were washed in PBS and suspended at hematocrit (Hct) of 10%. One mL of RBC suspension was applied to a 5 mL syringe attached to a Millex-HA membrane filter (Millipore, SLHA025BS) and pressurized manually at a rate of one drop/5 seconds until the filtration was stopped. The vesicles in the filtrate (~0.6 mL) were collected by centrifugation at 120,000 × g for 30 minutes at 4℃through a cushion of 20% sucrose in PBS and washed once in PBS. Vesicles were directly dissolved in 20 μL sample buffer for SDS-PAGE and stored frozen at −20℃until analysis by SDS-PAGE.

For decreasing the interactions between membrane skeleton and lipids, RBCs suspended in PBS were incubated for 30 minutes at 37℃in the presence or absence of 50 μM 4,4'-diisothiocyanostilbene-2,2'-disulfonate (DIDS; Cayman Chemical), washed and resuspended in PBS. [30]

Measurement of membrane mechanical properties

Deformability and mechanical stability of RBC membranes were examined as described previously.[31, 32]

Statistical analysis

All data are expressed as the mean ± S.D. Statistical significance was determined by using unpaired Student *t* tests, one-way analysis of variance (ANOVA), or Mann-Whitney test as indicated in the legends, and differences with a value of *P*

< .05 were considered statistically significant. All statistical analyses were performed by using GraphPad Prism 9.0 (GraphPad).

Data sharing statement

For original data, please contact the corresponding author, Mutsumi Inaba (inazo@vetmed.hokudai.ac.jp). DNA sequences of bovine *SPTA1* and *SPTB* were deposited in GenBank™ with accession numbers OL303989 (SpαA), OL303990 (SpαB), OL303991 (SpαBK91), OL303992 (SpβA), and OL303993 (SpβB), respectively.

Analysis of cDNA and genomic DNA of bovine α- and β-spectrin, genotyping, preparation of plasmids, production of recombinant proteins and their characterization are described in the supplemental Methods.

Results

Two distinct RBC phenotypes in bovine band 3 deficiency

We first demonstrated that band 3-deficient cattle homozygous for the R664X mutation of *SLC4A1* can be clearly divided into two groups, type 1 and type 2 (Figure 1A–1C). Both type 1 and type 2 RBCs showed spherocytosis and anisocytosis, with little noticeable difference in morphology (Figure 1A). However, incubation at ambient temperature for several hours, approximately 70% of type 1 RBCs had prominent blebs and protrusions under phase-contrast microscopy, whereas no such obvious vesicle extrusion was seen in the RBCs from type 2 and control animals (Figure 1B–1C).

The membranes from type 1 RBCs showed a marked reduction in the major membrane skeletal proteins, spectrin, 4.1R, and actin, along with the total lack of band 3 and protein 4.2, as reported previously.[14] Spectrin content was markedly reduced to 49.7% ± 3.8% (mean ± S.D., n = 3, $P < 0.01$) of control membranes (mean ± S.D., 100.0% ± 4.4%, n = 3). The Triton shells from type 1 RBCs also showed a marked reduction in the content of membrane skeletal proteins. However, type 2 band 3-deficient animals showed no apparent reduction in membrane skeletal proteins in both RBCs and Triton shells: the spectrin content in RBC membranes was similar to that in control membranes (mean ± S.D., 106.7% ± 4.7%, n = 3, $P = 0.135$; Figure 1D). Interestingly, both types exhibited inclusion of albumin in the membrane fraction, indicating invagination of the RBC membrane.[14]

We tested whether vesicles released from type 2 band 3-deficient RBCs contained spectrin, as we previously reported for type 1 RBCs.[14] Because type 2

RBCs showed no spontaneous fragmentation, we mechanically induced RBC vesiculation. Compared to control RBCs, suspensions of the two different types of band 3-deficient RBCs had lesser resistance to filtration. Noticeably, however, the volume of vesicles obtained from type 2 RBCs was almost the same as that obtained from control RBCs and approximately one-fifth obtained from type 1 RBCs. Whereas vesicles from type 1 RBCs contained readily detectable amounts of α- and β-spectrin, vesicles from type 2 RBCs contained no appreciable amounts of spectrin and showed a protein profile very similar to that of vesicles from control RBCs, except for the absence of band 3 (Figure 1E).

These findings demonstrate that type 2 RBCs represent the predominant phenotype of band 3 deficiency, membrane surface area loss without significant reduction in membrane skeletal components, as reported in mouse models and human band 3 deficiency.[15, 16, 23, 24] Thus marked fragility of type 1 RBCs is a composite phenotype caused by band 3 deficiency and an additional defect.

Spectrin reduction and membrane instability in type 1 is due to E91K substitution in α-spectrin

We analyzed the exon sequences of the erythroid *SPTA1* in a control and one for each of type 1 and type 2 band 3-deficient cattle and found three independent alleles with different nucleotide sequences, SpαA, SpαB, and SpαBK91 (supplemental Figure 1). The SpαA and SpαB alleles produce α-spectrin isoforms A and B, respectively, that are distinct from each other at 14 amino acid residues (Figure 2A; supplemental Figure 1). The SpαBK91 allele contains an additional substitution in the SpαB backbone, generating the E91K variant of isoform B. The SpαBK91 was originally found in a type 1 band 3-deficient animal, and the following survey revealed that all band 3-deficient individuals with type 1 RBCs (n = 3) were heterozygous for the SpαBK91 allele, whereas no SpαBK91 allele was detected in individuals with type 2 RBCs (n = 3). Importantly, type 1 band 3-deficiency with heterozygous SpαBK91 were more anemic with larger decreases in Hct and hemoglobin values than type 2 band 3- deficiency which did not harbor the spectrin E91K substitution (Table 1), implying that the E91K substitution increased the clinical severity of spherocytosis due to band 3 deficiency.

To assess the impact of the E91K substitution independent of band 3 deficiency, we analyzed spectrin content and membrane mechanical properties of RBCs from healthy cattle with various *SPTA1* genotypes. Genotyping of 167 individuals for *SPTA1* (Figure 2A; supplemental Figure 2) showed that SpαA and SpαB were the major alleles in both Japanese black and Holstein Friesian cattle. The SpαBK91 allele was only seen in Japanese black cattle with an allele frequency of ~15%. Quantification of the relative abundance of spectrin showed that spectrin

content was reduced by ~15%, in RBC membranes homozygous and heterozygous for K91 α-spectrin (K/K and E/K, respectively; Figure 2B; supplemental Figure 3), compared with the membranes containing only E91 α-spectrin (E/E; Figure 2B). Comparison among different *SPTA1* genotypes further showed that spectrin was also decreased in RBCs from individuals with SpαB/SpαBK91 and SpαBK91/SpαBK91 genotypes (B/BK91 or B91K/B91K), compared with SpαB/SpαB RBCs (B/B; Figure 2C). The E91K substitution is thus the dominant factor in reducing spectrin content.

Ektacytometry analysis revealed that the DI values increased with increasing applied shear stress for red cells with normal band 3 of all three genotypes E/E, E/K, and K/K with E/E RBCs showed a difference in DI curve at low shear stress possibly due to tumbling of RBCs.[33, 34] Interestingly, the maximal DI values for K/K and E/K RBCs were similar and higher than E/E RBCs (Figure 2D). In terms of membrane mechanical stability, K/K and E/K RBCs readily fragmented under high sheer stress conditions (750 dyn/cm^2), reaching minimum DI values within 20 seconds, whereas E/E RBCs fragmented gradually over 100 seconds (Figure 2E), implying the E91K substitution is the dominant determinant of membrane mechanical stability. Taken together with the lack of significant differences in mRNA levels among different *SPTA1* genotypes (supplemental Figure 4), the allele-specific reduction in spectrin is attributable to impaired assembly of the membrane skeleton.

Despite marked instability of RBC membranes *in vitro* under non-physiologically high shear forces, the individuals possessing K91 α-spectrin showed no noticeable abnormalities in RBC morphology and red cell indices (supplemental Figure 5), implying that fragmentation and loss of membrane components due to E91K substitution proceeds slowly under physiological conditions in the circulation.

Disordered structure of the α1 repeat due to E91K substitution

To investigate how the E91K substitution affects the mechanical stability of the membranes, we assessed the impact of the E91K substitution on the structure of recombinant bovine α[0–1] and α–β-fused mini-spectrins (Figure 3A). Structure prediction of bovine α[0–1] by the Phyre2 server[35] depicted a domain structure similar to its human counterpart in both the unbound[36] and bound[22] states with no notable difference in the overall structure between α[0–1]E91 and α[0–1]K91 (Figure 3B–3C), although several changes due to the E91K substitution were suggested in the vicinity of the E91K substitution site in α[0–1]K91, including the disappearance of interhelical hydrogen bonds shown for the bound state of α[0–1]E91 (Figure 3D).

The CD of α[0–1]E91 showed typical α-helical secondary structure with an α-helix content of 56.3%, whereas α[0–1]K91 had decreased α-helix content of 46.7%, indicating some unfolding due to E91K substitution. Reduction in α-helix content was

also apparent in mini-SpK91 (Figure 4A). The thermal denaturation profile of α[0–1]E91 revealed clear cooperative transition from an α-helical to a disordered structure between 46°C to 60°C with a transition mid-point (T_m) of ≃ 54°C, consistent with the previously reported T_m for α1[37, 38] or α[0–1][14] of human α-spectrin. In contrast, α[0–1]K91 showed a reduced ellipticity even at 25°C and an almost linear decrease with no discriminate transition in ellipticity from 25°C to 70°C, reflecting progressive unfolding (Figure 4B). The thermal denaturation of mini-SpE91 exhibited at least two transitions, first T_m at ≃ 43°C followed by the second at ≃ 51°C suggesting cooperative multistate unfolding. Notably, mini-SpK91 showed markedly reduced ellipticities from 25°C to 60°C with a clear helical-to-random transition with T_m ≃ 43°C which corresponded to the first transition for mini-SpE91, implying that the E91K substitution destabilizes local structure of α[0–1] without significant structural alterations in distal repeats.

In the ^{1}H-^{15}N HSQC spectra at 25°C, numerous signal peaks were distributed evenly in the spectra for both ^{15}N-α[0–1]E91 and ^{15}N-α[0–1]K91 (Figure 4C). However, less dispersion of chemical shifts was apparent for ^{15}N-α[0–1]K91. At 40°C, most of the signal peaks were lost in the spectrum for ^{15}N-α[0–1]K91, consistent with the reduced thermal stability of α[0-1]K91 in CD analysis. Notably, Hε-Nε signals presumably derived from two conserved tryptophan residues (W59 and W131) observed for ^{15}N-α[0–1]E91 disappeared in the ^{15}N-α[0–1]K91 spectrum (^{1}H, 10.2–10.5 ppm; ^{15}N, 125–126 ppm), indicating less ordered structure in α1 region of α[0–1]K91 in the vicinity of K91 and spatially adjacent conserved tryptophan residues likely involved in hydrophobic interhelical interactions[39, 40] (Figure 3D).

Fluorescence spectra from W59 and W131 in α1 and the susceptibility of the fluorescence intensity to a hydrophilic collisional quencher acrylamide were analyzed. α[0–1]E91 and α[0–1]K91, as well as their W59F mutants, showed fluorescence spectra with the maximum emission intensity wavelength (λ_{max}) of 330–340 nm and reduction in the fluorescence intensities by the addition of acrylamide in a concentration-dependent manner (Figure 4D). The K_{SV} values for α[0–1]K91 and α[0–1]K91/W59F were significantly higher than those for α[0–1]E91 and α[0–1]E91/W59F, respectively (Figure 4E–4F). In contrast, α[0–1]E91/W131F and α[0–1]K91/W131F showed blue shifts of λ_{max} to ~330 nm and their K_{SV} values were nearly equal to each other (Figure 4D–4F). Therefore, tryptophan residues in α[0–1]K91 and α[0–1]K91/W59F are more susceptible to acrylamide compared with those in their counterparts containing E91,[41–43] indicating higher exposure of the W131 residue presumably due to destabilization of α1.

Collectively, these data indicate that the E91K substitution causes structural destabilization greater than predicted (Figure 3B–3D), including unfolding and unwinding in the triple-helical bundle of the α1 domain.

E91K substitution reduces spectrin tetramer formation which is worsened by perturbation of band 3–ankyrin linkage

To unravel how the disordered α1 leads to the impaired membrane skeletal organization, we assessed the effect of E91K substitution on oligomer states of α–β fused mini-spectrin "dimers" as previously described.[44] Purified "tetramer (dimers of α–β-fused mini-spectrin)" fractions, with a Stokes radius of ~80 Å, of SpE91 and SpK91 were collected and concentrated. Following incubation at 37℃ for 1 hour, mini-SpE91 and mini-SpK91 eluted in two peaks corresponding to the tetramer (80 Å) and dimer (54 Å) fractions (Figure 5A). The relative abundance of the tetramer in mini-SpK91 was markedly lower than that in mini-SpE91 (the means ± S.D., 38.9% ± 18.6% *vs.* 86.6% ± 8.0%, n = 3, $P < 0.05$; Figure 5B). The 1:1 mixture of mini-SpE91 and min-SpK91 also showed intermediate values between that of either species (68.9% ± 11.5%, n = 3), indicating that the tetramer containing mini-SpK91 is less stable and more readily dissociated to dimer than that formed by mini-SpE91.

Finally, we examined the impact of the loss of membrane bilayer–skeleton linkage, characteristic of band 3 deficiency, on the stability of RBC membranes with reduced spectrin tetramerization by treatment of RBCs with DIDS which reduces band 3-ankyrin association[30] (Figure 5C–5H; supplemental Figure 6). Vesicles obtained from E/E and E/K RBCs by filtration-induced hemolysis contained band 3 and negligible amount of spectrin (Figure 5C–5D). Similarly, vesicles generated by E/E RBCs treated with DIDS prior to filtration had negligible content of spectrin. Importantly, the vesicles obtained from DIDS-treated E/K RBCs contained remarkable amount of spectrin (Figure 5C–5G) and also the junctional complex constituent 4.1R (Figure 5H), suggesting local fragmentation of the membrane skeleton and release of its components into the vesicles.

These data demonstrate that the E91K substitution impairs the mechanical stability of the membrane skeleton through reduced spectrin tetramerization and that disturbing the membrane–membrane skeletal association exacerbates the membrane loss.

Discussion

The present study showed that weakened spectrin tetramerization due to the E91K substitution in α-spectrin markedly exacerbates spherocytic phenotypes due to band 3 deficiency. Generation of spectrin-free vesicles in filtration-induced hemolysis from type 2 band 3-deficient RBCs without E91K substitution, as well as those from control RBCs (E/E RBCs), indicated that the membrane skeleton in type 2 spherocytes was nearly intact. In marked contrast, in type 1 band 3-deficient RBCs

possessing E91K substitution, increased dissociation of spectrin tetramers into dimers causes local accumulation of disrupted spectrin skeleton and consequent release of the membrane vesicles containing fragmented membrane skeleton including spectrin and 4.1R. Thus HS in type 1 RBCs with extremely fragile membranes, originally reported for bovine band 3 deficiency,[14] is caused by combined phenotypes involving the surface area loss due to complete lack of band 3 and as well as membrane fragmentation due to impaired spectrin self-association, features of HS and HE, respectively.[12, 13, 21] Thus, the E91K substitution in bovine α-spectrin is a novel *SPTA1* allele-specific modulator of membrane defects including band 3 deficiency.

Notably, however, E/K and K/K RBCs with reduced spectrin tetramerization but normal band 3 contents did not show significant hematological lesions, although these cells exhibited marked mechanical instability under non-physiologically high shear force in ektacytometry, suggesting that these RBCs possess some mechanism(s) that limits the damage due to altered spectrin tetramerization. Spectrin tetramerization occurs through head-to-head binding of adjacent spectrin dimers connected to the junctional complex. Since the binding affinity between dimers is extremely low,[33, 45, 46] the probability of dimers encountering head-to-head is a major determinant for tetramer formation. If adjacent dimers connected to the junctional complex are bound to the lipid bilayer through band 3–ankyrin association, the spatial movement of the dimer heads could be significantly restricted, promoting the self-association of spectrin dimers. Such a contribution of the band 3–ankyrin–spectrin linkage in spectrin tetramer formation was originally suggested by Morrow and Marchesi.[25] This hypothesis has been strengthened by the findings on the positively cooperative interaction between spectrin, ankyrin, and band 3[26] and the dissociation of a large proportion of spectrin tetramers into dimers by disrupting the spectrin–ankyrin–band 3 link.[27]

Our analysis also showed that membrane fractions prepared from type 2 band 3-deficient RBCs, but not from E/K and K/K RBCs, contained the plasma protein albumin indicating that the surface area loss in band 3 deficiency involves endocytic invagination followed by exocytic extrusion of microvesicles, as we previously reported for type 1 RBCs.[14] This process is very similar to the release of exosomes in membrane remodeling during reticulocyte maturation.[47, 48] Since band 3 is not contained in the exosomes released and remains totally associated with the RBC membrane during reticulocyte maturation,[49] exosome formation and thus exosome-like microvesicle formation in band 3-deficient RBCs appear to occur in membrane compartments lacking band 3. It will be interesting to determine whether such invagination is the consequence of an inward membrane curvature imposed by

altered transmembrane protein–lipid interactions[11] or occurs through the interaction of such membranes with the spectrin skeleton as a scaffolding machinery.[50]

A significant finding of the present study is that the E91K substitution in the α1 domain affects the function of the adjacent dimer–dimer self-association site. While many HE-associated α-spectrin mutations have been mapped to the partial repeat α0,[12] some HE mutations are located distant from the critical tetramerization site, mainly the linkers joining helices C and A or the C-terminal region of helix C adjacent to the linker.[12, 22, 38] The only exception reported to date is the common L207P mutation in the α2 domain,[51, 52] which is located in the middle of helix B as is the case for E91K. The L207P mutation, as well as another common HE-associated mutation L260P, has been shown to cause no extensive unfolding but shift the dimer–tetramer equilibrium towards closed dimers due to alterations in the triple-helical bundle of α2 to a more compact and stable structure, resulting in reduced and destabilized formation of spectrin tetramers.[6, 53] In contrast, the E91K substitution appears to cause unfolding of α-helices and destabilization accompanied by unwinding of the triple-helical bundle in α1, suggesting a mechanism different from that for L207P mutation to reduce self-association of dimers. Intriguingly, in human α-spectrin, α0 is connected to α1 with a flexible linker in the unbound state and these regions are stabilized by forming a continuous α-helical structure consisting of α0, helix A in α1, and the linker region between α0 and α1 upon binding with β-spectrin.[22, 36] The tertiary state of the α1 domain with E91K substitution implies disturbed conformational change of α[0–1] or perturbation of proper relative positioning of β16, β17/α0, and α1 repeats required in tetramer formation.[22] Moreover, the disordered structure of α1 may lead to the impairment of the supposed interstrand interactions of α1 (at K70 and E125/E126 in the vicinity of the E91K substitution site) with α2–α3 repeats in the parallel strand of α-spectrin within the tetramer.[6] The prediction by the MutationExplorer software (http://proteinformatics.org/mutation_explorer/)[54] shows that the relevant mutation E100K in human α[0–1] causes structural destabilization with ΔΔG values of −2.78 and −6.47 in unbound and bound states, respectively, indicating that similar destabilization of spectrin tetramerization is expected in human RBCs. However, we still need to consider its potential effect on the allosteric effect of spectin-ankyrin association to spectrin dimer self-association,[26] which could not be evaluated in our tetramer formation experiment using mini-spectrin proteins. Further kinetic and molecular dynamic studies for the interactions between band 3, ankyrin, and intact spectrin variants in red cells and in solutions would be required to precisely determine the mechanism for destabilized tetramer formation due to E91K substitution, in turn the physiology of spectrin tetramer stabilization by the band 3–membrane skeleton link.

In summary, our findings on naturally occurring cases of a novel substitution E91K in bovine *SPTA1*, in combination with the band 3 deficiency-causative *SLC4A1* mutation, substantiate the long-standing hypothesis on an important role for band 3–ankyrin–spectrin linkage in maintaining the mechanical properties of the RBC membrane, in addition to its well-established function in stabilizing the membrane lipid bilayer. The findings also imply that combination of different membrane protein mutations working in conjunction can account for variable clinical severity of red cell membrane disorders including HS.

Acknowledgments

We thank Akira Ban, Mikio Konno, Kenji Wada, Jun-ichi Sakai, and Yoshimi Ogata (Yamagata Prefectural Federation of Agricultural Mutual Relief Association) and Kazutaka Iwata (Iwata Animal Clinic) for collection of blood samples; Wataru Otsu, Daisuke Ito, Kota Sato, Keitaro Morishita, Takashi Kikukawa, and Momoko Fujimoto (Hokkaido University) for technical support; Kimiko Ito (Tokyo Women's Medical University) for ektacytometry; Mitsuhito Matsumoto and Satoshi Tamahara (University of Tokyo) for technical support; Ken-ichiro Ono (University of Tokyo) for intellectual support; and Makoto Nakao and the late Sumie Manno (Tokyo Women's Medical University), and the late Wataru Nunomura (Tokyo Women's Medical University and Akita University) for constructive discussion.

This study was supported in part by Grants-in-aid for Scientific Research 15658096, 16H05031, 20H03138, and 23K27065 from the Japan Society for Promotion of Science (to M. I.) and DK32094 from NIH (to M. N.).

Authorship

Contribution: M. I. designed the research; K. M., M. T., T. T., O. I., and M. I. designed experiments, performed experiments, and analyzed the data; N. A., I. K., and Y. O.-Y. performed experiments and analyzed the data; M. D. analyzed the data; K. K., A. K., and E. K. performed experiments; K. M., M. T., and M. I. wrote the original manuscript; N. M., Y. T., and M. I. analyzed the data, made critical intellectual contributions throughout the research, and edited the manuscript.

Disclosure of conflicts of interest: All authors declare no competing financial interests.

The current affiliation for E.K. is Jichi Medical University.

Footnotes

Current address: K. M., Research Center, Mochida Pharmaceutical Co., Ltd., Gotemba 412-0047, Japan; M. T., Graduate School of Veterinary Science, Osaka Metropolitan University, Osaka 598-8531, Japan; and Y. O.-Y., Division of Biomedical Information Analysis, Iwate Tohoku Medical Megabank Organization, Iwate Medical University, Iwate 028-3609, Japan

References

1. Chasis JA, Mohandas N. Erythrocyte membrane deformability and stability: Two distinct membrane properties that are independently regulated by skeletal protein associations. *J Cell Biol.* 1986; 103(2): 343–350.
2. An X, Lecomte MC, Chasis JA, et al. Shear-response of the spectrin dimer–tetramer equilibrium in the red blood cell membrane. *J Biol Chem*. 2002; 277(35): 31796–31800.
3. Mohandas N, Gallagher PG. Red cell membrane: past, present, and future. *Blood.* 2008; 112(10): 3939–3948.
4. Lux SE IV. Anatomy of the red cell membrane skeleton: unanswered questions. *Blood.* 2016; 127(2): 187–199.
5. Liu S-C, Derick LH, Palek J. Visualization of the hexagonal lattice in the erythrocyte membrane skeleton. *J Cell Biol.* 1987; 104(3): 527–536.
6. Sriswasdi S, Harper SL, Tang H-Y, et al. Probing large conformational rearrangements in wild-type and mutant spectrin using structural mass spectrometry. *Proc Natl Acad Sci USA.* 2014; 111(5): 1801–1806.
7. Bennett V, Stenbuck PJ. The membrane attachment protein for spectrin is associated with band 3 in human erythrocyte membranes. *Nature.* 1979; 280(5722): 468–473.
8. Anderson RA, Lovrien RE. Glycophorin is linked by band 4.1 protein to the human erythrocyte membrane skeleton. *Nature.* 1984; 307(5952): 655–658.
9. Salomao M, Zhang, X, Yang Y, et al. Protein 4.1R-dependent multiprotein complex: new insights into the structural organization of the red blood cell membrane. *Proc Natl Acad Sci USA.* 2008; 105(23): 8026–8031.
10. Low PS, Willardson BM, Mohandas N, et al. Contribution of band 3–ankyrin interaction to erythrocyte membrane mechanical stability. *Blood.* 1991; 77(7): 1581–1586.

11. Van Dort HM, Knowles DW, Chasis JA, et al. Analysis of integrated membrane protein contributions to deformability and stability of the human erythrocyte membrane. *J Biol Chem.* 2001; 276(50): 46968–46974.
12. Gallagher PG. Hereditary elliptocytosis: Spectrin and protein 4.1R. *Sem Hematol.* 2004; 41(2), 142–164.
13. Perrotta S, Gallagher PG, Mohandas N. Hereditary spherocytosis. *Lancet.* 2008; 372(9647), 1411–1426.
14. Inaba M, Yawata,A, Koshino I, et al. Defective anion transport and marked spherocytosis with membrane instability caused by hereditary total deficiency of red cell band 3 in cattle due to a nonsense mutation. *J Clin Invest.* 1996; 97(8): 1804–1817.
15. Peters LL, Shivdasani RA, Liu S-C, et al. Anion exchanger 1 (band 3) is required to prevent erythrocyte membrane surface loss but not to form the membrane skeleton. *Cell.* 1996; 86(6): 917–927.
16. Southgate CD, Chishti AH, Mitchell B, et al. Targeted disruption of the murine erythroid band 3 gene results in spherocytosis and severe haemolytic anaemia despite a normal membrane skeleton. *Nat Genet.* 1996; 14(2): 227–230.
17. Inaba M, Maede Y. A new major transmembrane glycoprotein, gp155, in goat erythrocytes. Isolation and characterization of its association to cytoskeleton through binding with band 3-ankyrin complex. *J Biol Chem.* 1988; 263(33): 17763–17771.
18. Ito D, Koshino I, Arashiki N, et al. Ubiquitylation-independent ER-associated degradation of an AE1 mutant associated with dominant hereditary spherocytosis in cattle. *J Cell Sci.* 2006; 119(17): 3602–3612.
19. Sato K, Otsuka Y, Arashiki N, et al. Identification of genes for two major sialoglycoproteins, glycophorin A and glycophorin C in canine red cell membranes. *Jpn J Vet Res.* 2008; 55(4): 103–114.
20. Chen Y, Miyazono K, Otsuka Y, et al. Membrane skeleton hyperstability due to a novel alternatively spliced 4.1R can account for ellipsoidal camelid red cells with decreased deformability. *J Biol Chem.* 2023; 299(2), 102877.
21. Gaetani M, Mootien S, Harper S, et al. Structural and functional effects of hereditary hemolytic anemia-associated point mutations in the alpha spectrin tetramer site. *Blood.* 2008; 111(12): 5712–5720.
22. Ipsaro JJ, Harper SL, Messick TE, et al. Crystal structure and functional interpretation of the erythrocyte spectrin tetrameization domain complex. *Blood.* 2010; 115(23), 4843–4852.
23. Ribeiro ML, Alloisio N, Almeida H. et al. Severe heresitary spherocytosis and distal tubular acidosis associated with the total absence of band 3. *Blood*. 2000; 96(4): 1602–1604.

24. Bruce L, Beckman R, Ribeiro ML, et al. A band 3-based macrocomplex of integral and peripheral proteins in the RBC membrane. *Blood*. 2003; 101(10): 4180–4188.
25. Morrow JS, Marchesi VT. Self-assembly of spectrin oligomers *in vitro*: a basis for a dynamic cytoskeleton. *J Cell Biol.* 1981; 88(2): 463–468.
26. Giorgi M, Cianci CD, Gallagher PG, et al. Spectrin oligomerization is cooperatively coupled to membrane assembly: a linkage targeted by many hereditary hemolytic anemias? *Exp Mol Pathol.* 2001; 70(3): 215–230.
27. Blanc L, Salomao M, Guo X, et al. Control of erythrocyte membrane-skeletal cohesion by the spectrin-membrane linkage. *Biochemistry.* 2010; 49(21): 4516–4523.
28. Liu S-C, Derick LH, Agre P, et al. Alteration of the erythrocyte membrane skeletal ultrastructure in hereditary spherocytosis, hereditary elliptocytosis, and pyropoikilocytosis. *Blood.* 1990; 76(1): 198–205.
29. Inaba M, Gupta KC, Kuwabara M, et al. Deamidation of human erythrocyte protein 4.1: possible role in aging. *Blood.* 1992; 79(12): 3355–3361.
30. Van Dort HM, Moriyama R, Low PS. Effect of band 3 subunit equilibrium on the kinetics and affinity of ankyrin binding to erythrocyte membrane vesicles. *J Biol Chem.* 1998; 273(24): 14819–14826.
31. An X, Takakuwa Y, Nunomura W, et al. Modulation of band 3-ankyrin interaction by protein 4.1. Functional implications in regulation of erythrocyte membrane mechanical properties. *J Biol Chem.* 1996; 271(52): 33187–33191.
32. Manno S, Takakuwa Y, Mohandas N. Identification of a functional role for lipid asymmetry in biological membranes: Phosphatidylserine-skeleton protein interactions modulate membrane stability. *Proc Natl Acad Sci USA.* 2002; 99(4): 1943–1948.
33. Hale J, An X, Guo X, et al. αI-spectrin represents evolutionary optimization of spectrin for red blood cell deformability. *Biophys J.* 2021; 120(17): 3588–3599.
34. Dupire J, Socol M, Viallat A. Full dynamics of a red blood cell in shear flow. *Proc Natl Acad Sci USA.* 2012; 109(51): 20808–20813.
35. Kelley LA, Mezulis S, Yates CM, et al. The Phyre2 web portal for protein modeling, prediction and analysis. *Nat Protocol.* 2015; 10(6): 845–858.
36. Park S, Caffrey MS, Johnson ME, et al. Solution structural studies on human erythrocyte α-spectrin tetramerization site. *J Biol Chem.* 2003; 278(24): 21837–21844.
37. An X, Guo X, Zhang X, et al. Conformational stabilities of the structural repeats of erythroid spectrin and their functional implications. *J Biol Chem.* 2006; 281(15): 10527–10532.

38. Johnson CP, Gaetani M, Ortiz V, et al. Pathogenic proline mutation in the linker between spectrin repeats: disease caused by spectrin unfolding. *Blood.* 2007; 109(8): 3538–3543.
39. Pantazatos DP, MacDonald RI. Site-directed mutagenesis of either the highly conserved Trp-22 or the moderately conserved Trp-95 to a large, hydrophobic residue reduces the thermodynamic stability of a spectrin repeating unit. *J Biol Chem.* 1997; 272(34): 21052–21059.
40. Brenner AK, Kieffer B, Travé G, et al. Thermal stability of chicken brain alpha-spectrin repeat 17: a spectroscopic study. *J Biomol NMR.* 2012; 53(2): 71-83.
41. Eftink MR, Ghiron CA. Exposure of tryptophanyl residues in proteins. Quantitative determination by fluorescence quenching studies. *Biochemistry.* 1976; 15(3): 672–680.
42. Vivian JT, Callis PR. Mechanisms of tryptophan fluorescence shifts in proteins. *Biophys J.* 2001; 80(5): 2093–2109.
43. Lakowicz JR. Protein fluorescence. In: Principles of fluorescence spectroscopy, 3rd ed, pp. 529-575, Springer, Baltimore, MA; 2006
44. Harper SL, Li D, Maksimova Y, et al. A fused α–β “mini-spectrin” mimics the intact erythrocyte spectrin head-to-head tetramer. *J Biol Chem.* 2010; 285(14): 11003–11012.
45. Ungewickell E, Gratzer W. Self-association of human spectrin. A thermodynamic and kinetic study. *Eur J Biochem.* 1978; 88(2): 379–385.
46. Salomao M, An X, Guo X, et al. Mammalian αI-spectrin is a neofunctionalized polypeptide adapted to small highly deformable erythrocytes. *Proc Natl Acad Sci USA.* 2006; 103(3): 643–648.
47. Johnston RM, Adam M, Hammond JR, et al. Vesicle formation during reticulocyte maturation. Association of plasma membrane activities with released vesciles (exosomes). *J Biol Chem.* 1987; 262(19). 9412–9420.
48. Johnston RM, Bianchini A, Teng K. Reticulocyte maturation and exosome release: transferrin receptor containing exosomes shows multiple plasma membrane functions. *Blood.* 1989; 74(5): 1844–1851.
49. Komatsu T, Arashiki N, Otsuka Y, et al. Extrusion of Na,K-ATPase and transferrin receptor with lipid raft-asspciated proteins in different populations of exosomes during reticulocyte maturation in dogs. *Jpn J Vet Res.* 2010; 58(1): 17–27.
50. Kim JH, Chen EH. The fusogenic synapse at a glance. *J Cell Sci.* 2019; 132(18): jcs214124.
51. Gallagher PG, Tse WT, Coetzer T, et al. A common type of the spectrin αI 46-50a-kD peptide abnormality in hereditary elliptocytosis and pyropoikilocytosis is

associated with a mutation distant from the proteolytic cleavage site. *J Clin Invest.* 1992; 89(3): 892–898.

52. Gallagher PG, Forget BG. Spectrin St. Louis and the α^{LELY} allele. *Blood.* 1994; 84(5). 1686–1687.
53. Harper SL, Sriswasdi S, Tang H-Y, et al. The common hereditary elliptocytosis-associated α-spectrin L260P mutation perturbs erythrocyte membranes by stabilizing spectrin in the closed dimer conformation. *Blood.* 2013; 122(17): 3045-3053.
54. Philipp M, Moth CW, Ristic N et al. MUTATIONEXPLORER: a webserver for mutation of proteins and 3D visualization of energetic impacts. *Nucl Acids Res.* 2024; 52(W1): W132–W139.

Table 1. Hematological parameters of band 3-deficient cattle with different red cell phenotypes

	Band 3-deficient Type 1*	Band 3-deficient Type 2*	Control (n = 19)**
RBC ($\times 10^{-6}$/μL)	4.3 ± 0.5	5.3 ± 0.3	7.2 ± 0.7
Hct (%)	23.3 ± 2.4	32.9 ± 2.2	37.1 ± 4.7
Hb (g/dL)	8.0 ± 0.9	11.5 ± 0.8	13.3 ± 1.6

MCV (fL)	54.9 ± 2.4	62.7 ± 3.5	51.6 ± 5.0
MCH (pg)	18.1 ± 0.8	21.9 ± 1.3	18.5 ± 1.8
MCHC (%)	34.3 ± 0.9	34.9 ± 1.0	35.9 ± 0.9
Reticulocyte (%)	< 0.1	< 0.1	< 0.1

RBC, red blood cell count; Hct, hematocrit; Hb, hemoglobin; MCV, mean corpuscular volume; MCH, mean corpuscular hemoglobin; and MCHC, mean corpuscular hemoglobin concentration.

*The mean ± S.D. of 13 repeated examinations for each individual between the ages of 4 and 6.

**The mean ± S.D. of 19 different examinations for individuals from age 1 to 6 years.

Legends for Figures

Figure 1. Two distinct RBC phenotypes of band 3 deficiency in cattle. (A–B) scanning electron micrographs (A) and phase-contrast micrographs (B) of RBCs from a healthy control cattle (*a*) and a type 1 (*b*) and a type 2 (*c*) band 3-deficient cattle. For scanning electron micrography shown in (A), whole blood cells were fixed with 1.0% glutaraldehyde in 0.1 M sodium phosphate (pH 7.4) within 1 hour after sampling. RBCs were suspended in PBS and allowed to stand at ambient temperature. After 6 hours, RBCs were examined under phase-contrast microscopy at 1,000× magnification (B) and the numbers of RBCs possessing prominent protrusions were counted. (C) The top panel indicates a magnification of the boxed area in panel (*b*) in (B). Data are shown in % of RBCs with protrusions in 200 RBCs and expressed as the means ± S.D. (n = 4). ****P < .0001 by one-way analysis of variance (ANOVA) with Tukey's multiple comparison test. *ns*, not significant. Bars indicate 6 μm (A), 20 μm (B), and 10 μm (C), respectively. (D) Ghost membranes (*Ghost*) were prepared from 1 × 10^8 RBCs obtained from a healthy normal animal (*Control*) and a type 1 (*B3-null 1*) and a type 2 (*B3-null 2*) band 3-deficient cattle. Membrane proteins were solubilized in 2% Triton X-100 and the insoluble fractions (*Triton shell*) were obtained by ultracentrifugation. Proteins in the ghosts and Triton shells were separated on 8% SDS-gels followed by staining with Coomassie brilliant blue. The bands indicated by an *open arrowhead* contain serum albumin in invagination-derived vesicles.[14] (E) Filtration-induced hemolysis generated fragmented vesicles in the filtrates. RBCs from the animals were pressurized on the membrane filter and the vesicles in the filtrate were collected by ultracentrifugation and washed once. Proteins in the vesicles were directly solubilized in the sample buffer for SDS-PAGE and half the volume of the

sample was loaded on 8% SDS-gels followed by staining with Coomassie blue. Note that the vesicles from type 1 RBCs were dissolved in five times the volume of buffer and one-tenth of the solubilized sample, that is equivalent to the volume of other samples, was applied to the well. α- and β-spectrin are apparent only in the vesicles from type 1 band 3-deficient RBCs (*arrowheads*). Migrating positions of α- and β-spectrin, band 3, 4.1R, 4.2, actin, and globins in ghost membranes, as well as those of size marker proteins shown in kDa, are indicated in (D) and (E).

Figure 2. The E91K variant α-spectrin causes marked reduction in spectrin contents and mechanical stability of RBC membranes. (A) Japanese black cattle (*JB*, n = 136) and Holstein Friesian cattle (*HF*, n = 31) were genotyped for the *SPTA1* alleles. All these animals were free from the premature termination mutation R664X, causative of band 3 deficiency in cattle. Alleles SpαA and SpαB, major alleles in both bovine species, are different in the nucleotide sequence, resulting in amino acid substitutions at 14 amino acid residues. The allele SpαBK91 has SpαB backbone and contains an additional nucleotide change which results in the E91K substitution. SpαBK91 was found only in Japanese black cattle so far examined. A minor allele SpαAB, possessing a chimeric sequence of SpαA and SpαB, was also found in both breeds during the process of genotyping. (B–C) RBC membrane proteins from Japanese black cattle (n = 136) were analyzed by SDS-PAGE and the abundance of spectrin relative to band 3 was determined by densitometric scanning. The data are summarized for the animals free from (*E/E*) and heterozygous (*E/K*) and homozygous (*K/K*) for E91K substitution in (B), or for different genotypes in (C). In (C), alleles SpαA, SpαB, SpαAB, and SpαBK91 are abbreviated as *A*, *B*, *AB*, and *BK91*, respectively. The data are indicated for each individual with the mean ± S.D. Sample numbers are shown in parentheses. Statistical significances were determined using Kruskal-Wallis ANOVA with Dunn's multiple comparison test; **P* < .05, and ***P* < .01. (D–E) Ektacytometry analysis for the expandability (D) and mechanical stability (E) of RBCs from animals with different E91K phenotypes. In (D), the data demonstrate the change in deformability index (DI) values of RBCs in response to increasing shear stress in rpm and expressed as the mean ± S.D. for *E/E* (n = 3) and *E/K* (n = 3). *K/K* represents independent samples (n = 2). Mann-Whitney test was used to calculate statistical significance between *E/E* and *E/K*; *****P* < .0001. The data in (E) indicate the change in DI values as a function of time under a high shear stress (750 dyn/cm^2). Representative data for *E/E* (n = 2), *E/K* (n = 1), and *K/K* (n = 1) RBCs are shown.

Figure 3. Domain structure of the N-terminal region of bovine α-spectrin with E91K substitution. (A) Domain structures of bovine spectrin recombinants used in this study, the N-terminal repeats, α[0-1] (*α[0–1]*), and mini-Sp, α[0–5]–β[16–17]

(*mini-Sp*), prepared according of bovine α[0–1] shown here represents that from the allele SpαB or SpαBK91 with whose difference in the 91st residue, E91 derived from SpαB and K91 from SpαBK91. The sequence is shown in alignment with that of the human RBC α[0–1], and the identical amino acid residues are indicated by asterisks. The 91st residue (*E91* or *K91*), two tryptophan residues (W59 and W131), and amino acid residues that differ between SpαA and SpαB alleles (E17/A17, H87/N87, and W139/Q139) are also indicated. Prediction of the secondary structure for bovine α[0–1] by the Jpred4 software (http://www.compbio.dundee.ac.uk/jpred4) showed its similarity to the structure that was determined by the solution NMR structural study for human α[0–1] (unbound state, PDB ID, 1OWA)[36] and by crystal structural study for α[0–1]–β[16–17] complex (bound state, PDB ID, 3LBX).[22] The α-helix *C'* in α0 and helices *A*, *B*, and *C* in α1 according to 1OWA are boxed in black rectangles, while the α-helices predicted for α[0–1]–β[16–17] complex according to 3LBX are shown in red rectangles. (B–C) Three-dimensional structures of bovine α[0–1]E91 (*α[0–1]E91*, shown in cyan) and α[0–1]K91 (*α[0–1]K91*, shown in salmon) predicted by the Phyre2 software[35] using 1OWA (B) or 3LBX (C) as templates. α-Helices C' in α0, and A, B, and C in α1 are indicated. The 91st amino acid residue E91 (*blue*) or K91 (*red*) and conserved specific side chains that make contact with β-spectrin at the interface of the dimer–dimer self-association[22] are shown with spheres and sticks, respectively. **D**, interhelical hydrogen bonds are depicted by the PyMOL software for the bound states of α[0–1]E91 (*left*) and α[0–1]K91 (*right*). Note that α[0–1]E91 contains interhelical hydrogen bonds involving E91–K63 and S96–W131 in the vicinity of the E91K substitution site (shown in magenta dotted lines), whereas these contacts are lost in α[0–1]K91.

Figure 4. The E91K substitution causes a remarkable structural alteration in α[0–1]. (A) CD wavelength scanning spectra for α[0–1] (*left panel*) having E91 (*α[0–1]E91*) or K91 (*α[0–1]K91*) and mini-Sp having E91 (*mini-SpE91, right panel*) or K91 (*mini-SpK91*). α[0–1] showed an α-helix content of 56.3%, whereas α[0–1]K91 had a less α-helix content (46.7%), (B) CD thermal stability analyses for the recombinant proteins shown in (A) at 222 nm. (C) NMR-^{1}H-^{15}N HSQC spectra of ^{15}N-α[0–1]E91 (*α[0–1]E91*) and ^{15}N-α[0–1]K91 (*α[0–1]K91*) at 25ºC (*left panel*) or 40ºC (*right panel*). The resonances from two tryptophan residues (W59 and W131) were detected only for α[0–1]E91 at 25ºC (*inserted figures*). (D) Representative emission spectra for α[0–1]E91 (*E91*) and α[0–1]K91 (*K91*) (*left panels*), α[0–1]E91/W59F (*E91/W59F*) and α[0–1]K91/W59F (*K91/W59F*) (*middle panels*), and α[0–1]E91/W131F (*E91/W131F*) and α[0–1]K91/W131F (*K91/W131F*) (*right panels*) in the presence of various concentrations of acrylamide (*0–250 mM*). (E) The data from each recombinant were fit to linear Stern-Volmer plot and K_{SV} value was calculated from the slope of the plot.

(F) The K_{SV} values for each recombinant were obtained from three independent measurements and are expressed as the means ± S.D. Fluorescence intensity is shown in arbitrary unit (*AU*). Statistical significance between *E91* and *K91* was calculated by unpaired Student *t* test; **P* < .05, ***P* < .01. *ns*, not significant. Statistical significance among the wild-type and variants of *E91* as well as the wild-type and variants of *K91* was determined by one-way ANOVA with Tukey's multiple comparison test; **P* < .05, ***P* < .01, ****P* < .001, *****P* < .0001.

Figure 5. Effects of the E91K substitution on mini-spectrin tetramerization and stability of the membrane skeleton. (A) Representative elution profiles of GPC for tetramer-dimer formation of mini-Sp. The mini-SpE91 (*E*) and mini-SpK91 (*K*) stored at 4ºC were incubated at 37ºC for 1 hour at a concentration of 0.2 mg/mL separately (*E/E* and *K/K*) or after 1:1 combined (*E/K*), chilled on ice for 10 minutes, and then loaded onto a Superdex 200 10/300 GL column. Eluting positions of tetramer (*T*), dimer (*D*), and marker proteins (thyroglobulin, 86 Å; ferritin, 61 Å; aldolase, 48 Å; ovalbumin, 28 Å) are indicated. (B) The abundance of the tetramer relative to the total amount of tetramer and dimer in GPC analysis in (A) are shown in % for each of *E/E*, *E/K*, and *K/K*. Data are expressed as the means ± S.D., n = 3. **P* < .05 by one-way ANOVA with Tukey's multiple comparison test. (C–D) Representative profiles of SDS-PAGE (C) and immunoblotting (D) to detect spectrin in vesicles generated from RBCs with or without DIDS treatment. RBCs from cattle with *SPTA1* genotypes SpαB/SpαB (*E/E*) or SpαB/SpαBK91 (*E/K*) were incubated in the presence (+) or absence (−) of 50 μM of DIDS at 37ºC for 30 minutes, washed and suspended in PBS, followed by filtration as described in the legend for Figure 1. Proteins in vesicles obtained (*Vesicle*) and RBC ghosts (*Ghost*) were separated by SDS-PAGE on 8% SDS-gels followed by staining with Coomassie brilliant blue (C) or immunoblotting using the anti-spectrin antibody (D). Migrating positions of α- and β-spectrin (*α-* and *β-Sp*), band 3 (*B3*), and size marker polypeptides in kDa are indicated. (E–G) The contents of band 3 (E) and spectrin (F, total of α and β) in vesicles obtained from filtrates of 1 mL 10% RBC suspension were determined by densitometric scanning of Coomassie blue-stained gels. The relative abundance of spectrin was shown as spectrin/band 3 in (G). Unpaired Student *t* test was used to determine statistical significance between E/E and E/K and between with or without DIDS treatment; ****P* < .001, *****P* < .0001. **H**, the vesicles from E/K RBCs (*E/K*) with (+) or without (−) DIDS treatment (described above) were analyzed for protein 4.1R by immunoblotting using the anti-4.1R antibody (*anti-4.1R*) in parallel with spectrin (*anti-Sp*). Signals for 4.1R (*4.1R*) and spectrin (*Sp*) and migrating positions of size markers in kDa are indicated.

Table 1. Hematological parameters of band 3-deficient cattle with different red cell phenotypes

	Band 3-deficient Type 1*	Band 3-deficient Type 2*	Control (n = 19)**
RBC (x 10^{-6}/μL)	4.3 ± 0.5	5.3 ± 0.3	7.2 ± 0.7
Hct (%)	23.3 ± 2.4	32.9 ± 2.2	37.1 ± 4.7
Hb (g/dL)	8.0 ± 0.9	11.5 ± 0.8	13.3 ± 1.6
MCV (fl)	54.9 ± 2.4	62.7 ± 3.5	51.6 ± 5.0
MCH (pg)	18.1 ± 0.8	21.9 ± 1.3	18.5 ± 1.8
MCHC (%)	34.3 ± 0.9	34.9 ± 1.0	35.9 ± 0.9
Reticulocyte (%)	< 0.1	< 0.1	< 0.1

RBC, red blood cell count; Hct, hematocrit; Hb, hemoglobin; MCV, mean corpuscular volume; MCH, mean corpuscular hemoglobin; and MCHC, mean corpuscular hemoglobin concentration.

*The mean ± S.D. of 13 repeated examinations for each individual between the ages of 4 and 6.

**The mean ± S.D. of 19 different examinations for individuals from age 1 to 6 years.

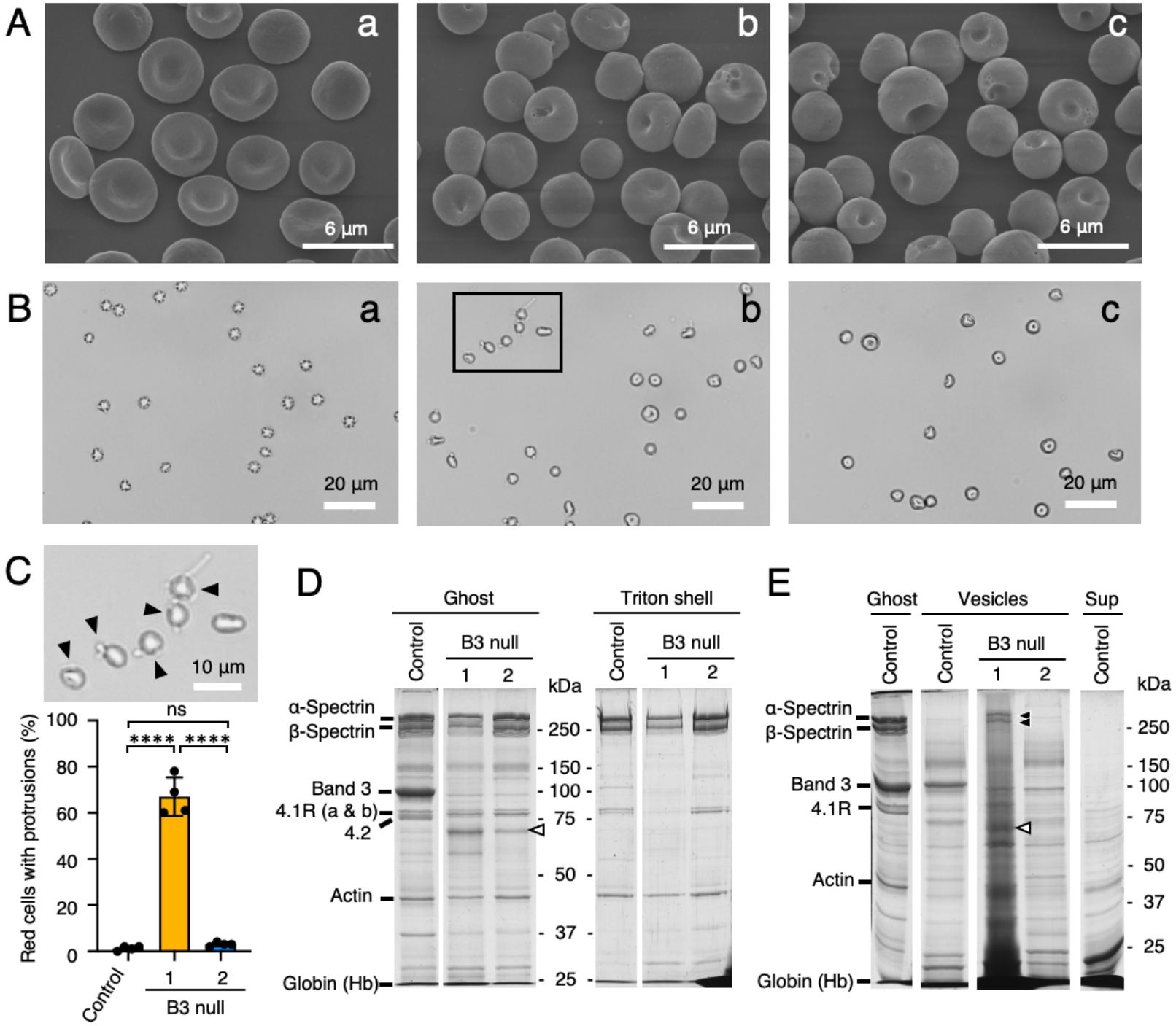
A
a
6 µm
b
6 µm
c
6 µm
B
a
20 µm
b
20 µm
c
20 µm
C
10 µm
ns
****
****
Red cells with protrusions (%)
100
80
60
40
20
0
Control
1
2
B3 null
D
Ghost
Triton shell
Control
B3 null
1
2
kDa
α-Spectrin
β-Spectrin
Band 3
4.1R (a & b)
4.2
Actin
Globin (Hb)
250
150
100
75
50
37
25
E
Ghost
Vesicles
Sup
Control
Control
B3 null
1
2
Control
kDa
α-Spectrin
β-Spectrin
Band 3
4.1R
Actin
Globin (Hb)
250
150
100
75
50
37
25

Figure 1

A

SPTA1 allele	Amino acid residues															Allele frequency	
	17	87	91	139	157	179	221	543	741	748	785	804	1086	1442	1585	JB (n = 136)	HF (n = 31)
SpαA	E	H	E	W	E	E	P	K	A	S	H	E	R	T	E	0.485	0.484
SpαB	A	N	E	Q	G	K	L	E	V	I	Y	V	H	A	A	0.335	0.468
SpαAB	E	H	E	W	E	E	P	K	V	I	Y	V	H	A	A	0.026	0.048
SpαBK91	A	N	K	Q	G	K	L	E	V	I	Y	V	H	A	A	0.154	0

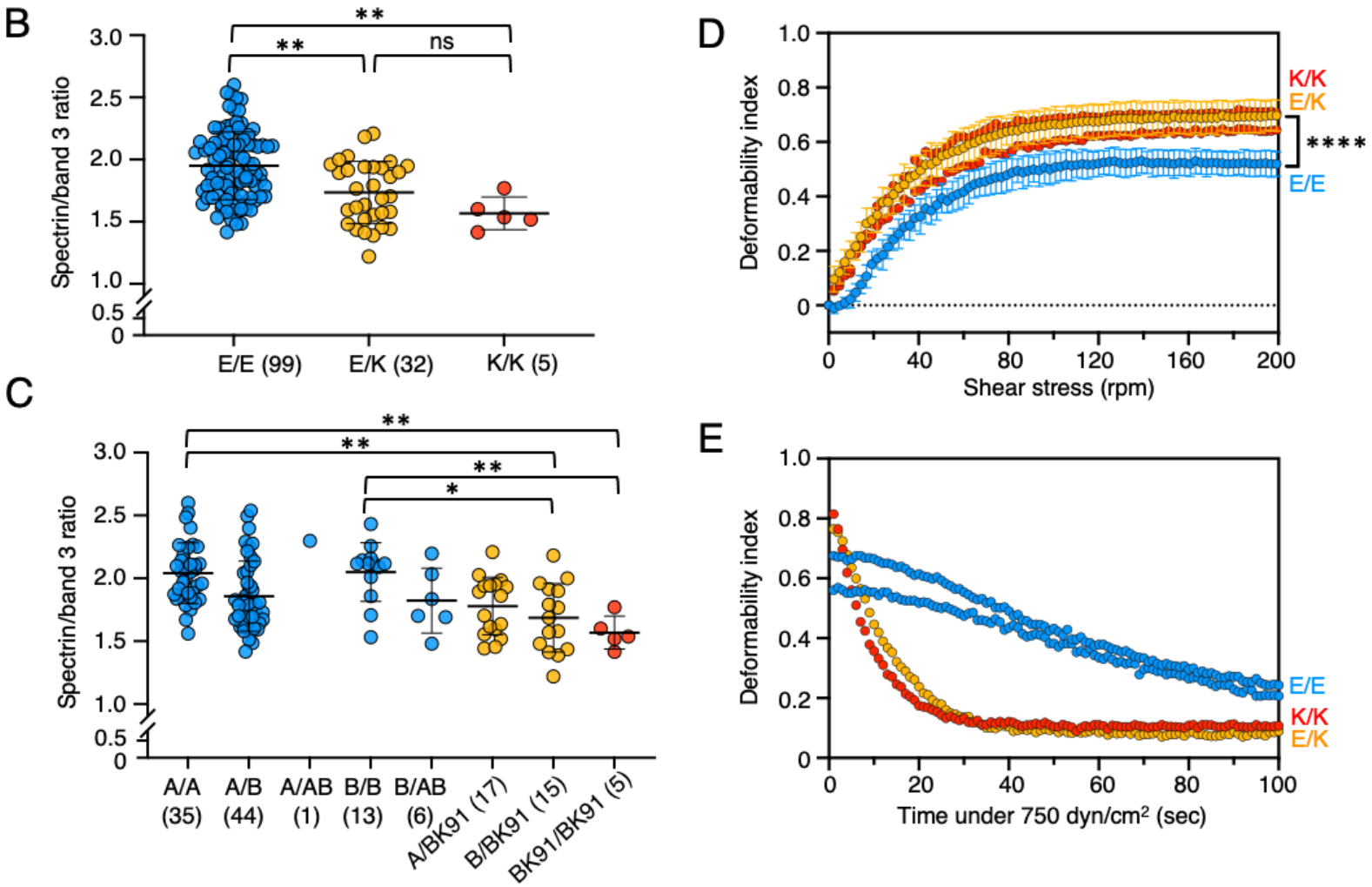

Figure 2

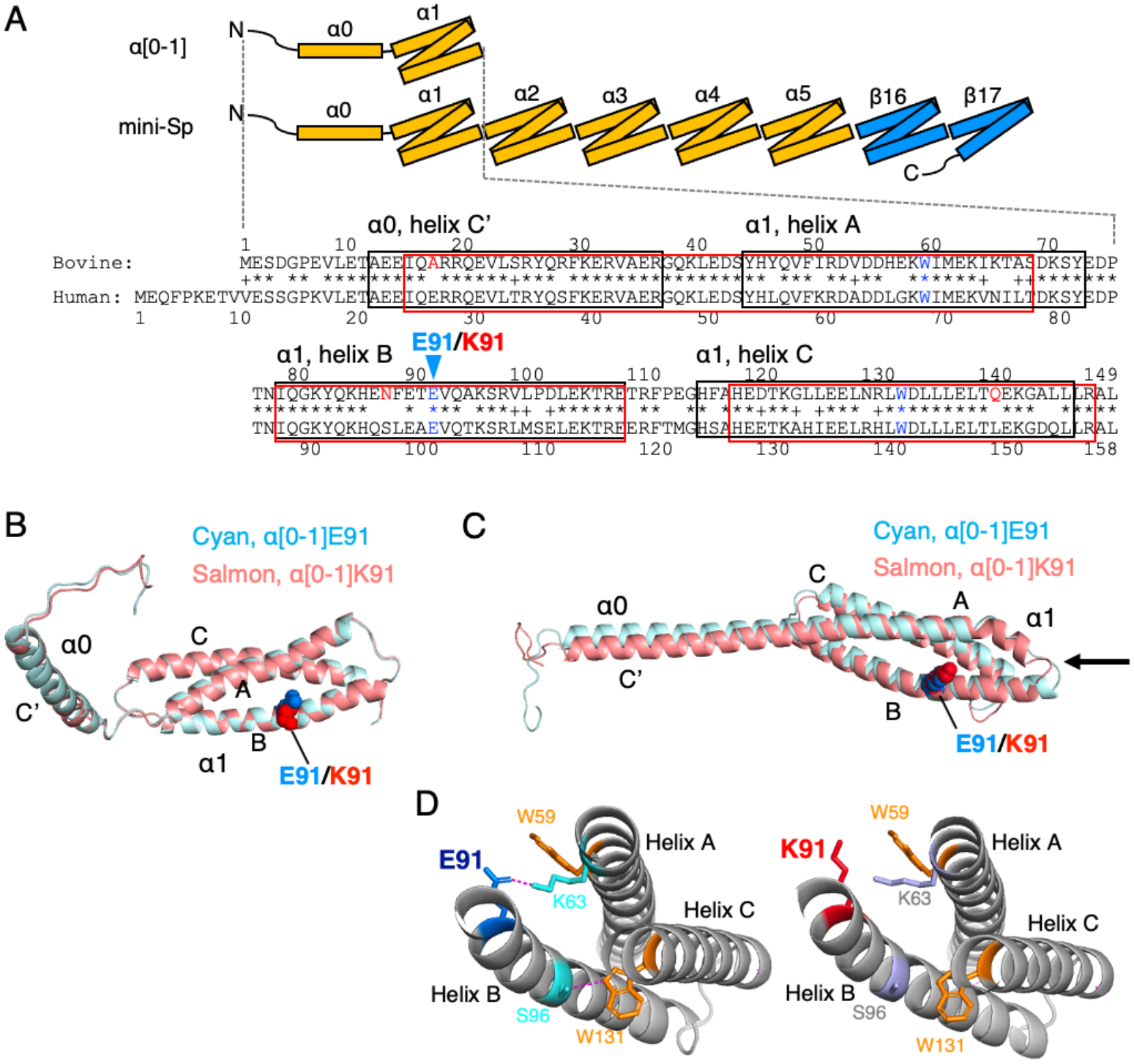
A
α[0-1]
mini-Sp
N
α0
α1
α2
α3
α4
α5
β16
β17
C
α0, helix C'
α1, helix A
α1, helix B
α1, helix C
E91/K91
Bovine:
Human:
B
Cyan, α[0-1]E91
Salmon, α[0-1]K91
C'
A
C
D
W59
K63
S96
W131
Helix A
Helix B
Helix C

Figure 3

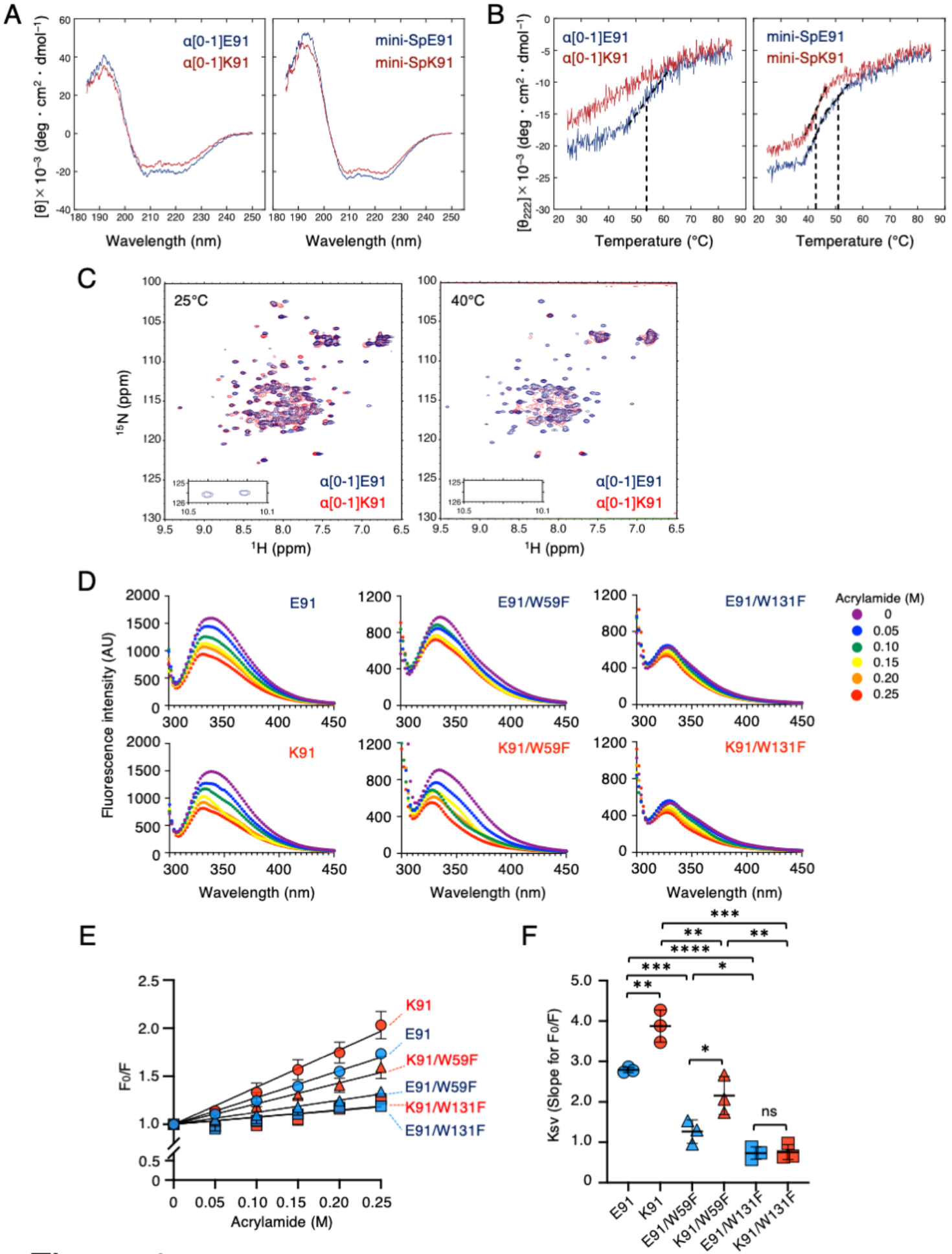
A
α[0-1]E91
α[0-1]K91
mini-SpE91
mini-SpK91
[θ] × 10⁻³ (deg · cm² · dmol⁻¹)
Wavelength (nm)
B
α[0-1]E91
α[0-1]K91
mini-SpE91
mini-SpK91
[θ222] × 10⁻³ (deg · cm² · dmol⁻¹)
Temperature (°C)
C
25°C
40°C
α[0-1]E91
α[0-1]K91
¹⁵N (ppm)
¹H (ppm)
D
E91
E91/W59F
E91/W131F
K91
K91/W59F
K91/W131F
Acrylamide (M)
0
0.05
0.10
0.15
0.20
0.25
Fluorescence intensity (AU)
Wavelength (nm)
E
K91
E91
K91/W59F
E91/W59F
K91/W131F
E91/W131F
F0/F
Acrylamide (M)
F
Ksv (Slope for F0/F)
ns
E91
K91
E91/W59F
K91/W59F
E91/W131F
K91/W131F

Figure 4

Figure 5-R1

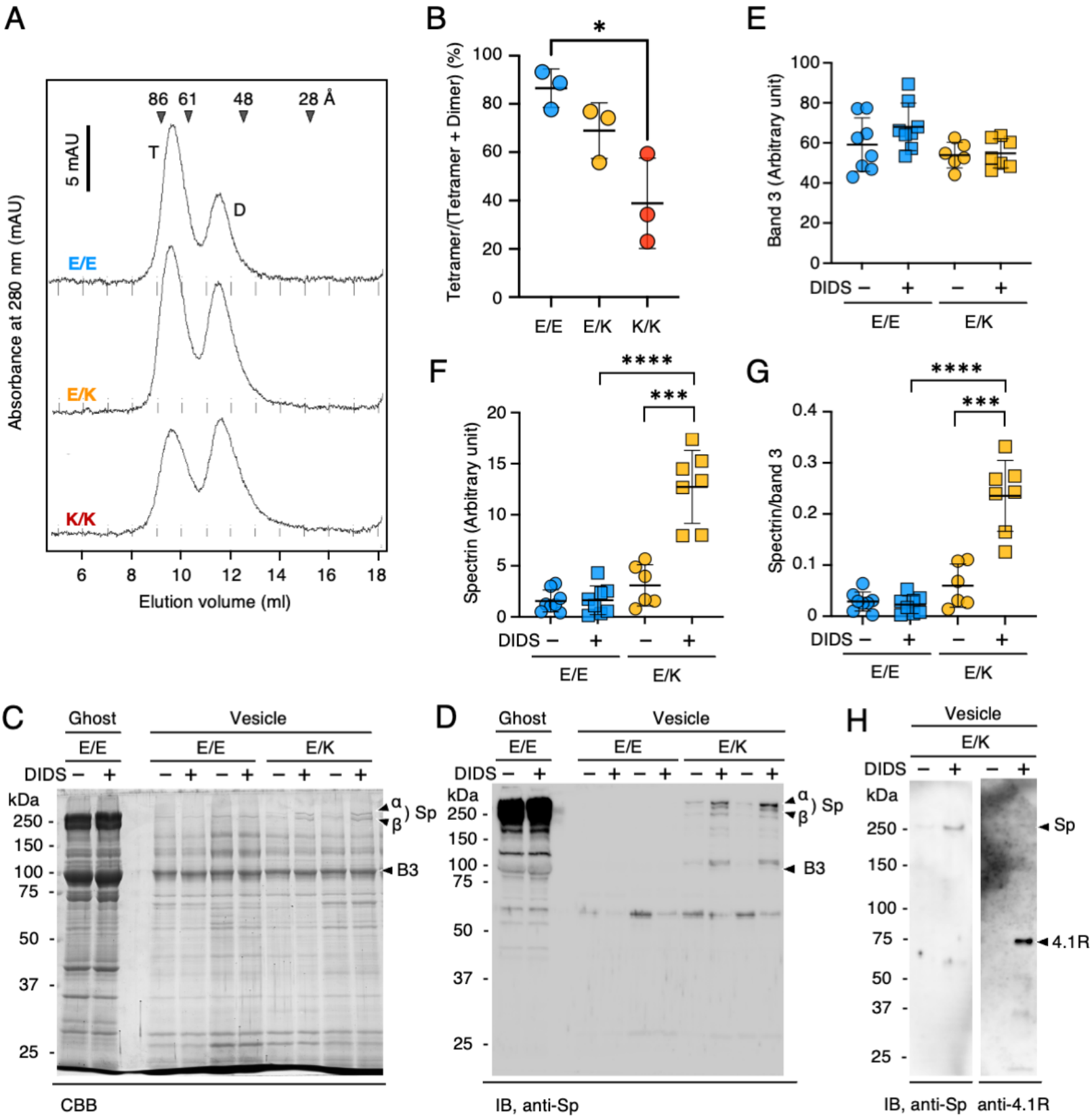

Figure 5

Supplemental Data

Red cell shape regulation by band 3–ankyrin–spectrin linkage: Implications for clinical severity of bovine HS

Kosuke Miyazono,[1] Mizuki Tomihari,[1, 2] Nobuto Arashiki,[1, 3] Ichiro Koshino,[2, 3] Yayoi Otsuka-Yamasaki,[1] Kota Kizaki,[1] Takashi Tsukamoto,[4] Osamu Inanami,[5] Ayumi Kawano,[1] Eri Kitaguchi,[1] Makoto Demura,[4] Narla Mohandas,[6] Yuichi Takakuwa,[3] and Mutsumi Inaba[1, 2, *]

[1]Laboratory of Molecular Medicine, Graduate School of Veterinary Medicine, Hokkaido University, Sapporo 060-0818, Japan; [2]Laboratory of Clinical Pathobiology, Graduate School of Agricultural and Life Sciences, University of Tokyo, Tokyo 113-8657, Japan; [3]Department of Biochemistry, School of Medicine, Tokyo Women's Medical University, Tokyo 162-8666, Japan; [4]Laboratory of Biological Information Analysis Science, Faculty of Advanced Life Science, Hokkaido University, Sapporo 060-0810 Japan; [5]Laboratory of Radiation Biology, Graduate School of Veterinary Medicine, Hokkaido University, Sapporo 060-0818, Japan; and [6]Red Cell Physiology Laboratory, New York Blood Center, New York, NY 10065

* Corresponding author: Mutsumi Inaba, Laboratory of Molecular Medicine, Faculty of Veterinary Medicine, Graduate School of Veterinary Medicine, Hokkaido University, Sapporo 060-0818, Japan. E-mail: inazo@vetmed.hokudai.ac.jp, Phone: +81-11-706-5580, Fax: +81-11-706-5276

Methods

Analysis of cDNA and genomic DNA of bovine α- and β-spectrin

Several overlapping segments as well as the 5'- and 3'-extended segments for α- and β-spectrin cDNAs from bone marrow cells from a healthy animal not carrying R664X mutation in *SLC4A1* were amplified by PCR and 5'- and 3'-RACE reactions using primers shown in supplemental Table 1. These primers were designed based on the nucleotide sequences of human *SPTA1* (GenBank accession number, NM_003126) and *SPTB* (GenBank accession number, J05500). At least six independent clones were isolated for each cDNA fragments and their nucleotide sequences were determined. The α- and β-spectrin cDNAs from one for each of type1 and type 2 band 3-deficient animals were obtained and sequenced using the same procedure.

These analyses demonstrated the presence of three independent alleles for *SPTA1*, namely SpαA, SpαB, and SpαBK91, that produce three different polypeptides of α-spectrin that differs each other at 14 or 15 amino acid residues. Likewise, two allelic sequences, namely SpβA and SpβB, were obtained for the bovine *SPTB*.

Genotyping

The *SPTA1* genotypes for E91K substitution and the *SPTA1* alleles, as well as the *SPTB* genotypes, were determined by PCR-RFLP using primer pairs and restriction enzymes listed in supplemental Table 1. Animals were also genotyped for the R664X mutation of *SLC4A1* as described previously.[1]

Preparation of recombinant protein-expressing plasmids

Several spectrin recombinants were prepared as GST-fused polypeptides. The cDNA for α[0–1]E91 (amino acid residues 1–147) was amplified from the bone marrow cDNA of an SpαB/SpαB genotype animal using a primer pair pSpaB01-3B and pSpaB01-4S (supplemental Table 1) and cloned into pGEX6P-1 (GE Healthcare) using *Bam* HI and *Sal* I sites to generate a bacterial expression vector pGEXSpα[0–1]E91. For construction of bovine "mini-spectrin" containing E91 (mini-SpE91), we followed a procedure reported by Harper et al.[2] Briefly, cDNA fragments for bovine α[0–5] (amino acid residues 1–575) with E91 and β[16–17] (amino acid residues 1,902–2,080) preceded by the linker with a sequence of GGGGGGIEGRGGGGGG were amplified by PCR using primers listed in supplemental Table 1, ligated at the *Eco* RI, and cloned into pGEX6P-1 using *Bam* HI and *Sal* I sites to create pGEXminiSpE91. The plasmids pGEXSpα[0–1]K91 and pGEXminiSpK91 for expression of GST-Spα[0–1]K91 and

GST-miniSpK91 were generated by mutagenesis of pGEXSpα[0–1]E91 and pGEXminiSpE91, respectively, by inverse PCR using mutagenic primers pSpaB-m9 and pSpaB-m10 (supplemental Table 1) followed by 5'-end phosphorylation and ligation.

Likewise, W59F and W131F mutants for each of GST-α[0–1]E91 and GST-α[0–1]K91 were also prepared by mutagenesis in pGEXSpα[0–1]E91 and pGEXSpα[0–1]K91, respectively. Mutations were generated by inverse PCR using mutagenic primers pSpaB-mW59FF and pSpaB-mW59FR for W59F and pSpaB-mW131FF and pSpaB-mW131FR for W131F mutations, respectively (supplemental Table 1).

Preparation of recombinant proteins

Production in BL21(DE)pLysS cells (Merck) and purification of GST-fused recombinant proteins were performed as reported previously.[3, 4] For NMR studies, α[0–1]E91 and α[0–1]K91 were labeled with ^{15}N as reported previously.[5–7] Briefly, transformed BL21(DE)pLysS cells were grown in M9-based medium in the presence of ^{15}N-ammonia water (SI Science Co., Saitama, Japan).

The GST-fused recombinant proteins including ^{15}N-labeled α[0–1] proteins were captured and digested with Turbo 3C protease (Wako Pure Chemical Industries, Osaka, Japan) to remove GST-tag on glutathione-Sepharose columns (GE Healthcare). Recombinant proteins in the eluates were dialyzed against a buffer consisting of 10 mM NaPi, pH 8.0, 2.5 mM EDTA and applied to a Mono Q column (GE Healthcare) equilibrated with the same buffer followed by a gradient elution with 1 M NaCl in the same buffer. Recombinant proteins were further purified on a gel permeation chromatography (GPC) column of Superdex 200 10/300 GL or Superdex 75 10/300 GL (both from Cytiva) in 10 mM NaPi, pH 7.4, 130 mM NaCl, and 1 mM EDTA. For circular dichroism (CD), NMR, and fluorescence spectroscopy, purified proteins were dialyzed and concentrated by ultrafiltration in 10 mM NaPi, pH 7.4.

CD and NMR spectroscopies

The CD spectra of α[0–1] and mini-Sp proteins (0.12 mM) were measured in the 185−250 nm region on a spectropolarimeter J-725 (JASCO, Tokyo, Japan) at 25°C. Then the thermal denaturation profile was obtained by CD change at 222 nm as a function of temperature from 25°C to 85°C at 1°C/minute. The α-helix content in the protein was estimated by a K2D3 program.[8]

The NMR samples (600 µl) contained 0.1 mM ^{15}N-labeled Spα[0–1] proteins, 10 mM NaPi, pH 7.4, and 10% (v/v) D_2O for the signal lock. ^{1}H-^{15}N HSQC NMR spectra were recorded on a 600 MHz spectrometer ECA600 (JEOL, Tokyo, Japan) equipped with a 5 mm triple resonance probe at 25°C and 40°C as reported previously for human

α[0–1].[7] The number of points for NMR measurements was set to 1,024 for the ^{1}H axis and 256 for the ^{15}N axis, and the number of integrations was set to 32.

Measurement of fluorescence spectra

The α[0–1] proteins and their W59F or W131F mutants (6.7 μM) were prepared in 10 mM NaPi, pH 7.4 in the presence or absence of appropriate concentrations of a fluorescence quencher acryladmide (Wako Pure Chemical Industries). Fluorescence spectra from tryptophan residues were measured on a fluorescence spectrophotometer F-2000 (Hitachi, Tokyo, Japan) with an excitation at 295 nm and 30°C. Fluorescence quenching by acrylamide was estimated as the Stern–Volmer constant (K_{SV}) in an equation $F_0/F = 1 + K_{SV}[Q]$ where F_0 is the fluorescence intensity in the absence of quencher, F is the fluorescence intensity, and [Q] is a quencher concentration in M.[9]

Analytical GPC

Purified mini-spectrins (mini-SpE91 and mini-SpK91) stored at 4°C were separated on a GPC column of Superdex 200 10/300 GL column equilibrated with 10 mM NaPi, pH 7.4, 130 mM NaCl, and 1 mM EDTA at 23°C and monitored at 280 nm. Mini-spectrins in fractions corresponding to “tetramers (dimers of α-β fused mini-spectrin)” with a Stokes radius of ~80 Å were collected and concentrated. Mini-SpE91 and mini-SpK91 were incubated at 37°C for 1 hour separately or mixed 1:1, chilled on ice for 10 minutes, then GPC was performed as described above.

Molecular modeling

Putative models of α[0–1]E91 and α[0–1]K91 were generated using the Phyre2 server (www.sbg.bio.ic.ac.uk/phyre2/html/).[10] The NMR solution structure of α[0–1] (PDB ID, 1OWA)[7] and the crystalized α[0–1] in the α[0–1]–β[16–17] complex (PDB ID, 3LBX)[11] were used as the templates. Images were modified using PyMOL graphics system (Schrödinger, Inc.).

References

1. Inaba M, Yawata,A, Koshino I, et al. Defective anion transport and marked spherocytosis with membrane instability caused by hereditary total deficiency of red cell band 3 in cattle due to a nonsense mutation. *J Clin Invest.* 1996; 97(8): 1804–1817.
2. Harper SL, Li D, Maksimova Y, et al. A fused α–β “mini-spectrin” mimics the intact erythrocyte spectrin head-to-head tetramer. *J Biol Chem.* 2010; 285(14): 11003–11012.
3. Otsuka Y, Ito D, Katsuoka K, et al. Expression of α-hemoglobin stabilizing protein and cellular prion protein in a subclone of murine erythroleukemia cell line MEL. *Jpn J Vet Res.* 2008; 56(2): 75–84.
4. Otsu W, Kurooka T, Otsuka Y, et al. A new class of endoplasmic reticulum export signal ΦXΦXΦ for transmembrane proteins and its selective interaction with Sec24C. *J Biol Chem.* 2013; 288(25): 18521–18532.
5. Uegaki K, Nemoto N, Shimizu M, et al. ^{15}N labeling method of peptides using a thioredoxin gene fusion expression system: an application to ACTH-(1-24). *FEBS Lett.* 1996; 379(1): 47–50.
6. Park S, Liao X, Johnson ME, et al. Letter to the editor: 1H, 15N, and 13C NMR backbone assignments of the N-terminal region of human erythrocyte alpha spectrin including one structural domain. *J Biomol NMR.* 1999; 15(4): 345–346.
7. Park S, Caffrey MS, Johnson ME, et al. Solution structural studies on human erythrocyte α-spectrin tetramerization site. *J Biol Chem.* 2003; 278(24): 21837–21844.
8. Louis-Jeune C, Andrade-Navarro MA, Perez-Iratxeta C. Prediction of protein secondary structure from circular dichroism using theoretically derived spectra. *Proteins.* 2012; 80(2): 374–381.
9. Gogami Y, Ito K, Kamitani Y, et al. Occurrence of D-serine in rice and characterization of rice serine racemase. *Phytochemistry.* 2009; 70(3): 380–387.
10. Kelley LA, Mezulis S, Yates CM, et al. The Phyre2 web portal for protein modeling, prediction and analysis. *Nat Protocol.* 2015; 10(6): 845–858.
11. Ipsaro JJ, Harper SL, Messick TE, et al. Crystal structure and functional interpretation of the erythrocyte spectrin tetrameization domain complex. *Blood.* 2010; 115(23), 4843–4852.

Table 1. Primers used in the present study

Gene	GenBank	Primer ID	Sequence (position)	Purpose
Cloning				
Human *SPTA1*	M61877	hSpAp1	5'-AGAGGGGTCAGAAGCTTGAGG-3' (104–124)	Cloning of bovine SPTA1 cDNA
		hSpAp2	5'-TGATCTTCTCTTCCTGGGCAG-3' (1570–1550)	
		hSpAp3	5'-AAGCCCTTCTTCAGAAGCATG-3' (1508–1528)	
		hSpAp4	5'-AGCATGTCTCCTGCCTCATAG-3' (3257–3237)	
		hSpAp5	5'-ATCGGGCAGAAGAACGCAGAC-3' (3179–3199)	
		hSpAp6	5'-GCCTGATCTTTCATGGCCAGC-3' (4880–4860)	
		hSpAp7	5'-AGCATCCGGGACTTTGAGTTC-3' (4816–4836)	
		hSpAp8	5'-GAAGCCAACGTAGTCATAGCC-3' (7203–7183)	
Human *SPTB*	J05500	hSpBp1	5'-TGCTGACATGACATCGGCCAC-3' (−7–13)	Cloning of bovine SPTB cDNA
		hSpBp2	5'-CTCGGTGAACTTCAGGGTGGC-3' (1788–1768)	
		hSpBp3	5'-ATCCAAGGGGACAAAGTGAAG-3' (1735–1755)	
		hSpBp4	5'-GTGAGCCAGAGTGTATTCCTG-3' (3579–3559)	
		hSpBp5	5'-TTCCAGAAAGATGCCAAGCAG-3' (3517–3537)	
		hSpBp6	5'-AAGAGTCACGTGGTCAAAGTC-3' (5181–5161)	
		hSpBp7	5'-TCAGACTTCAGGGGCAAGTGG-3' (4985–5055)	
		hSpBp8	5'-CTTCCTCCTCTTGAGGCCCAG-3' (6286–6266)	
Bovine *SPTA1*	OL303989 (SpαA)	SpAp9	5'-GAGGACATGAAGCAGGCCCTAACCCCAG-3' (7087–7114)	Cloning of bovine SPTA1 cDNA, 3'RACE
		SpAp10	5'-CCAGCAGCAGGTCCCACAGGCGGTTCAG-3' (406–379)	Cloning of bovine SPTA1 cDNA, 5'RACE
Bovine *SPTB*	OL303992 (SpβA)	SpBp9	5'-CAGCCGGGACTATGGACACACGGTGGAC-3' (6098–6125)	Cloning of bovine SPTB cDNA, 3'RACE
		SpBp10	5'-CCAGCTCATCATCCGGGCCGTCCCAGCG-3' (91–64)	Cloning of bovine SPTB cDNA, 5'RACE
Quantitative RT-PCR				
Bovine *SPTA1*	OL303089 (SpαA)	SpAp11	5'-TCTTATGGGTACCAGCGGTTC-3' (1078–1098)	Quantitative PCR for SPTA1 mRNA
		SpAp12	5'-CCACCAGTCACATCTATGGGC-3' (1187–1167)	
		SpAp13	5'-AGCAATCATTATGCCTCCGAC-3' (1921–1941)	
		SpAp14	5'-ACTGGATCCCTTTCTGCTCTG-3' (2020–2000)	
		SpAp15	5'-TCTGAAGACCACTATGCCAAG-3' (4357–4377)	
		SpAp16	5'-TGGTCCTTGAAGTCATGGTAG-3' (4508–4488)	
		SpAp17	5'-GCCAGGTCATTGGCTGTTTGG-3' (5707–5727)	
		SpAp18	5'-TCCAGGCCTCAACCACATCAG-3' (5797–5777)	
Bovine *SPTB*	OL303992 (SpβA)	SpBp11	5'-ACAGAACAACAGCCTCGAGGTC-3' (−232–−212)	Quantitative PCR for SPTB mRNA
		SpBp12	5'-CATTGATCCGGCTGTACGGTG-3' (61–41)	
		SpBp13	5'-ATCCAAGGGGACAAAGTGAAG-3' (1735–1755)	
		SpBp14	5'-CTTACAGAGCTGCTTGGACTG-3' (1923–1903)	
		SpBp15	5'-TTCCAGAAAGATGCCAAGCAG-3' (3517–3537)	
		SpBp16	5'-GTGAGCCAGGGTATATTCCTG-3' (3579–3559)	
		SpBp17	5'-GCGGAAGGAAAGCAGCTGATG-3' (4000–4020)	
		SpBp18	5'-TTGTGTGTTGGCCTGAAGCTC-3' (4107–4087)	

Bovine α-globin (*HBA*)	NM_001077422	HBAp1	5'-GACCAACTTCAAGGCCGCC-3' (58–81)	Internal standard for Quantitative PCR
		HBAp2	5'-AGGGTCACCAGCAGGGAGTG-3' (368–349)	
Genotyping				
Bovine band 3 (*SLC4A1*)	NM_181036	beb3p17	5'-AAACTCAGTGTACCTGAAGGC-3'	PCR-RFLP for band 3 R664X mutation
		beb3p14	5'-GCAAACATCATCCAGATGGGA-3'	
Bovine *SPTA1*	OL303989 (SpαA), OL303990 (SpαB), and OL303991 (SpαBK91)	SpAp49	5'-ATCATCCAGGAGACCAGGCTC-3' (intron 2)	PCR-RFLP for E91K substitution
		SpA54	5'-AATGCCCCTCAGGAAATCGAG-3' (exon 3)	
		SpAp19	5'-CTCTGGTGACATCAATGGAGC-3'	PCR-RFLP for E179K substitution
		SpAp58	5'-TCTGCACACTCATTGGCATATTG-3'	
		SpAp57	5'-ACCATAGACAAGACTGCAACCAAAC-3'	PCR-RFLP for K543E substitution
		SpAp60	5'-TCATCCCGGATAGCAGCGATC-3'	
		SpAp53	5'-GACCTTTTCCACCTGTACCAGATC-3'	PCR-RFLP for E804V substitution
		SpAp44	5'-CAAGGTAGGTGGAAGCCACTG-3'	
Bovine *SPTB*	OL303992 (SpβA) and OL303993 (SpβB)	SpBE3p1	5'-GCAATGGCGTCCCTCAGC-3'	PCR-RFLP for R124G substitution
		SpBE3p2	5'-GACCCACCTGGAAGCGCA-3'	
		SpBE11p3	5'-GAGCTGGAGCGGGAGAACTAC-3'	PCR-RFLP for M527T substitution
		SpBE11p4	5'-TTGATCCCGTCCATCCAGTCA-3'	
		SpBE22p1	5'-ATTGACTGCCAGGACGTGGAG-3'	PCR-RFLP for R1576Q substitution
		SpBE22p2	5'-GTTCTCGTCGGAGAAGACGTAGAA-3'	
Plasmid construction				
Bovine *SPTA1*	OL303990 (SpαB)	pSpaB01-3B	5'-AACCGCTGGATCCATGGAGAGTG-3'	pGEXSpα[0–1]E91, pGEXminiSpE91
		pSpaB01-4S	5'-GTCGACCCGCAGCAGCAGCAAGGCACCCTTC-3'	pGEXSpα[0–1]E91
		pSpaB05-6E	5'-GAATTCCAGAAGGAATGAATCCTCCAGC-3'	pGEXminiSpE91
		pSpaB-m9	5'-GAAACA**AAG**GTGCAAGCAAGCAAAATCAAGGG-3'	pGEXSpα[0–1]K91, pGEXminiSpK91
		pSpaB-m10	5'-AAAGTTTTCATGCTTCTGATATTTCCCC-3'	
		pSpaB-mW59FF	5'-**TC**ATCATGGAGAAAATCAAGACTGC-3'	pGEXSpα[0–1]E91/W59F, pGEXSpα[0–1]K91/W59F
		pSpaB-mW59FR	5'-**A**TTTCTCATGGTCATCAACATCTCG-3'	
		pSpaB-mW131FF	5'-**TC**GACCTGCTGCTGGAGCTGACCCA-3'	pGEXSpα[0–1]E91/W131F, pGEXSpα[0–1]K91/W131F
		pSpaB-mW131FR	5'-**A**CAGGCGGTTCAGTTCCTCCAGAAG-3'	
Bovine *SPTB*	OL303992 (SpβA)	pSpb1617-1E	5'-GAATTCGGTGGTGGTGGTGGTGGT**ATCGAAGGTCGT**GGTGGTGGTGGTGGTGGTACCGCAGACAAATTCCGCTTC-3'	pGEXminiSpE91
		pSpb1617-2S	5'-GTCGACTACTGGCGCTCTTTGAGCTC-3'	

Underlined: sequences for creating Bam HI, Sal I, or Eco RI restriction sites; Bold: sequences for mutagenesis, E91K, W59F, and W131F; Underlined bold: IEGR = FXa cleavage site.

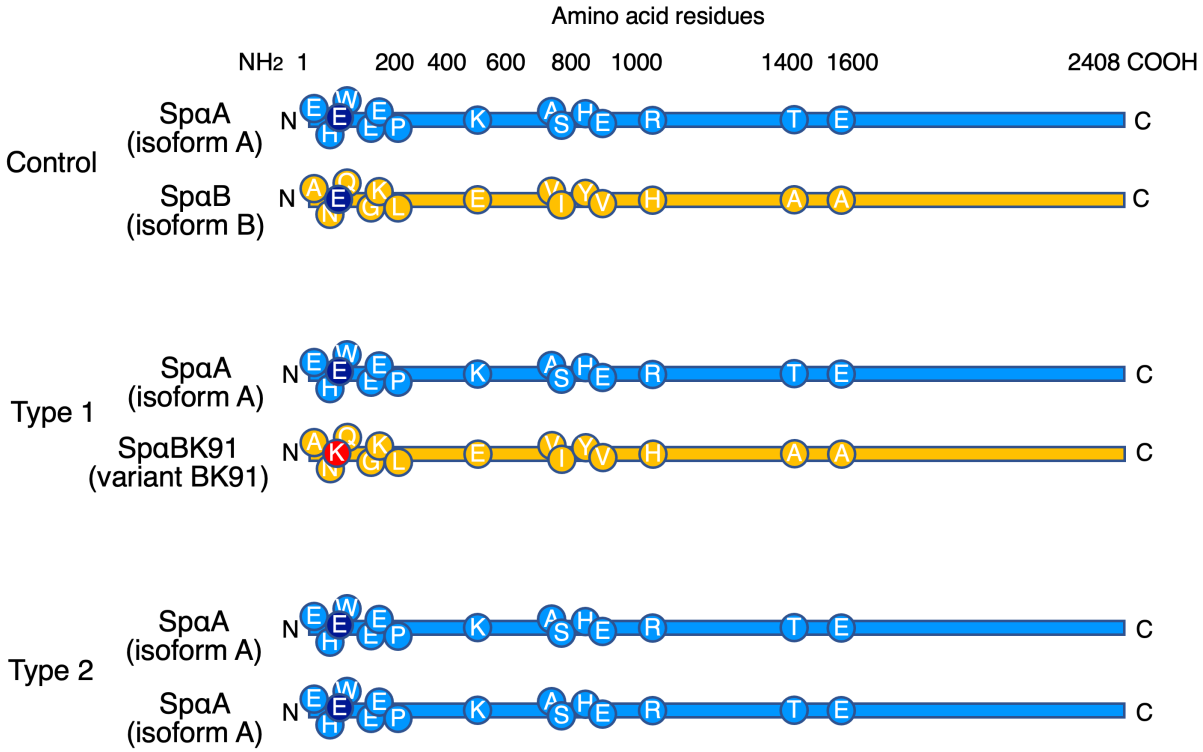

Figure 1. Diversity in the bovine *SPTA1* generating several distinct α-spectrin isoforms. The schema illustrates several distinct bovine α-spectrin isoforms A, B, and BK91, generated from *SPTA1* alleles, namely SpαA, SpαB, and SpαBK91, resepctively. These three alleles were identified by sequencing analyses of cDNAs and genomic DNAs from three individuals involving a control animal (*Control*) free from the R664X mutation, the causative of bovine band 3-deficiency,[1] and a type 1 (*Type 1*) and a type 2 (*Type 2*) band 3-deficient cattle. The isoforms A and B encoded by alleles SpαA and SpαB, respectively, are shown in blue and yellow, respectively. A variant BK91 carries an E91K substitution (allele SpαBK91) with a backbone of isoform B. Amino acid residues different among isoforms (shown in Figure 2A) are indicated in a single letter abbreviation and the E91K substitution is shown in red. DNA sequences of bovine *SPTA1* were deposited in GenBank™ with accession numbers OL303989 (SpαA), OL303990 (SpαB), and OL303991 (SpαBK91).

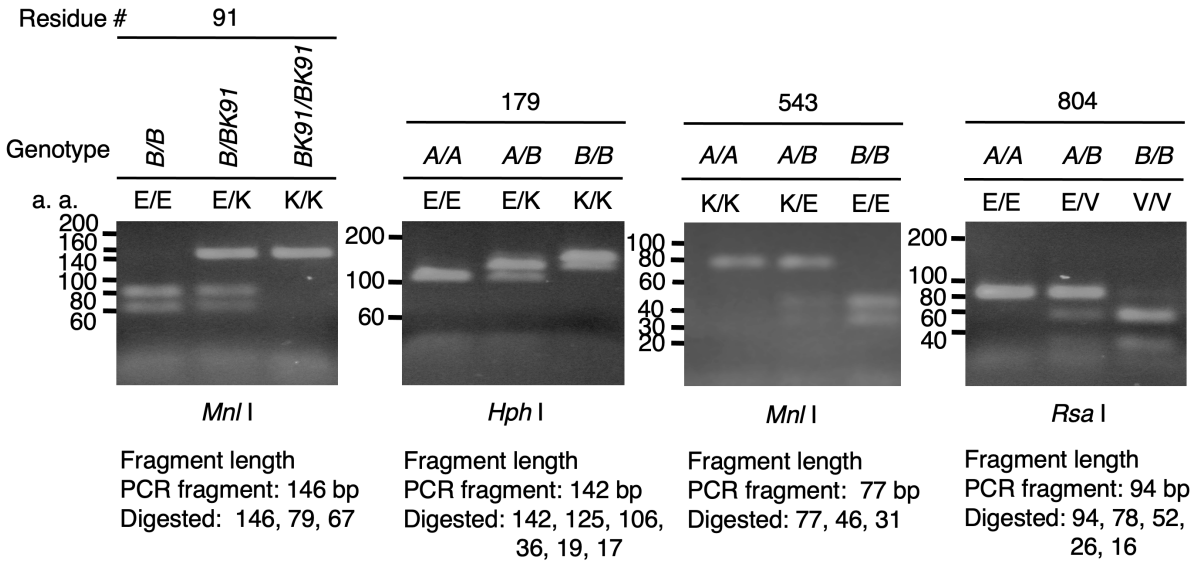

Figure 2. Genotyping of bovine *SPTA1* by PCR-RFLP. Animals were genotyped for *SPTA1* alleles by PCR-RFLP for variation of some amino acid residues. Genomic DNAs were amplified by PCR followed by digestion of the generated fragments with *Mnl* I (for the amino acid residues 91 and 543), *Hph* I (amino acid residue 179), and *Rsa* I (amino acid residue 804). Primer sequences for PCR are listed in supplemental Table 1. Genotypes due to allelic combinations, SpαA/SpαA, SpαA/SpαB, and SpαB/SpαB, are indicated as *A/A*, *A/B*, and *B/B* for the residues 179, 543, and 804, respectively. Amino acid residues (*a.a.*) according to genotypes are shown in single letter abbreviations such as *E/E*, *E/K*, *E/V*, *etc*. Genotyping for E91K substitution (E91 is derived from the SpαA and SpαB alleles, and K91 is derived from the SpαBK91 allele) is exemplified for individuals with SpαB/SpαB (*B/B*), SpαB/SpαBK91 (*B/BK91*), and SpαBK91/SpαBK91 (*BK91/BK91*) genotypes. Fragment lengths of PCR products with or without restriction enzyme digestion and migrating positions of size markers are shown in bp.

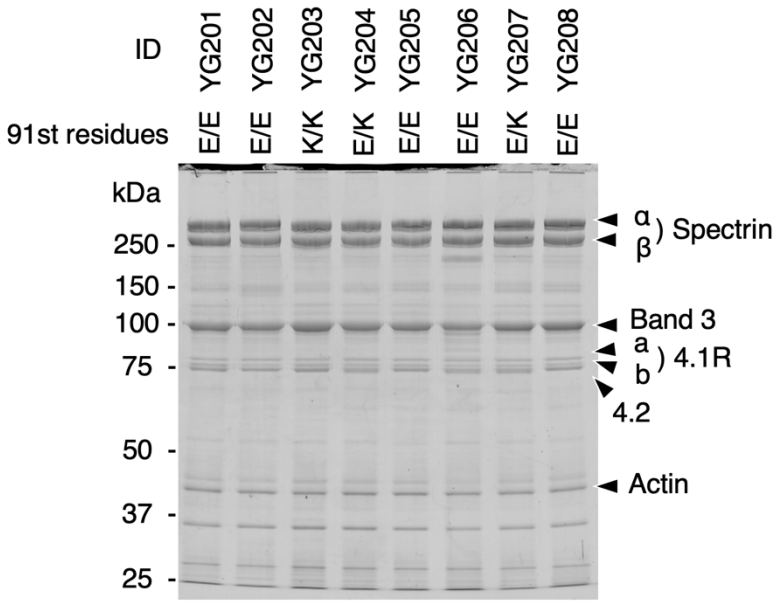

Figure 3. Representative SDS-PAGE profiles of RBC membrane proteins. RBC membrane proteins from Japanese black cattle (n = 136) were separated on 8% SDS-gels and stained with Coomassie brilliant blue to determine the relative abundance of spectrin as described in the text and Figure 2. A representative profile is shown here for 8 individuals, *ID YG201* to *YG208*, with different E91K phenotypes (*91st residues*, *E/E*, *E/K*, and *K/K*). The major membrane proteins and the migrating positions of size marker proteins in kDa are indicated.

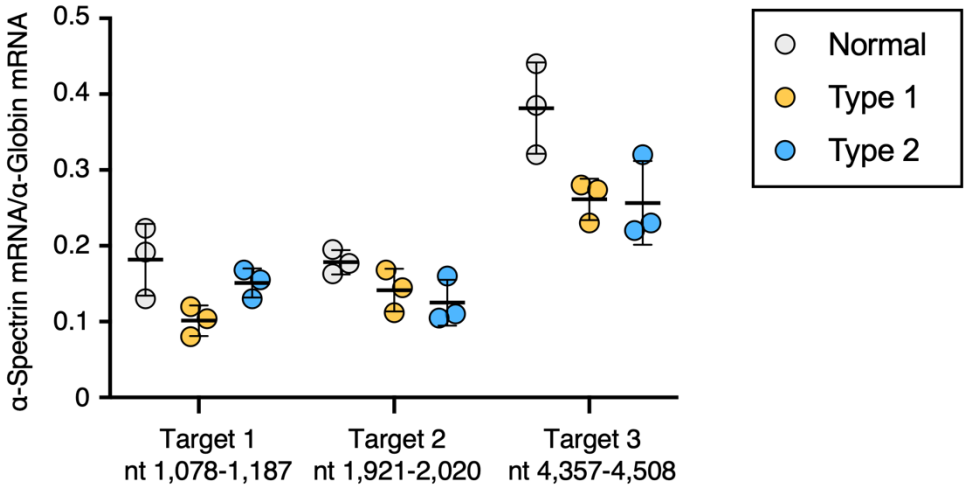

Figure 4. Relative abundance of α-spectrin mRNA in bone marrow cells. The levels of mRNA expression from *SPTA1* in bone marrow cells were analyzed by quantitative RT-PCR and normalized with those of α-globin mRNA (GenBank accession numbers, AJ242797, AJ242798, and AJ242799) for normal animal free from band 3 deficiency-causative mutation (*gray circles*) and type 1 (*yellow circles*) and type 2 (*blue circles*) band 3-deficient cattle shown in Figure 1. Quantitative RT-PCR was performed on three different sequences in α-spectrin mRNA, namely target 1 (nt 1,078–1,187), target 2 (nt 1,921–2,020), and target 3 (nt 4,357–4,508). Nucleotide sequences of the primers are listed in supplemental Table 1. Data are shown as the means ± S.D. (n = 3). No statistically significant difference was found among the individuals by Kruskal-Wallis one-way ANOVA analysis.

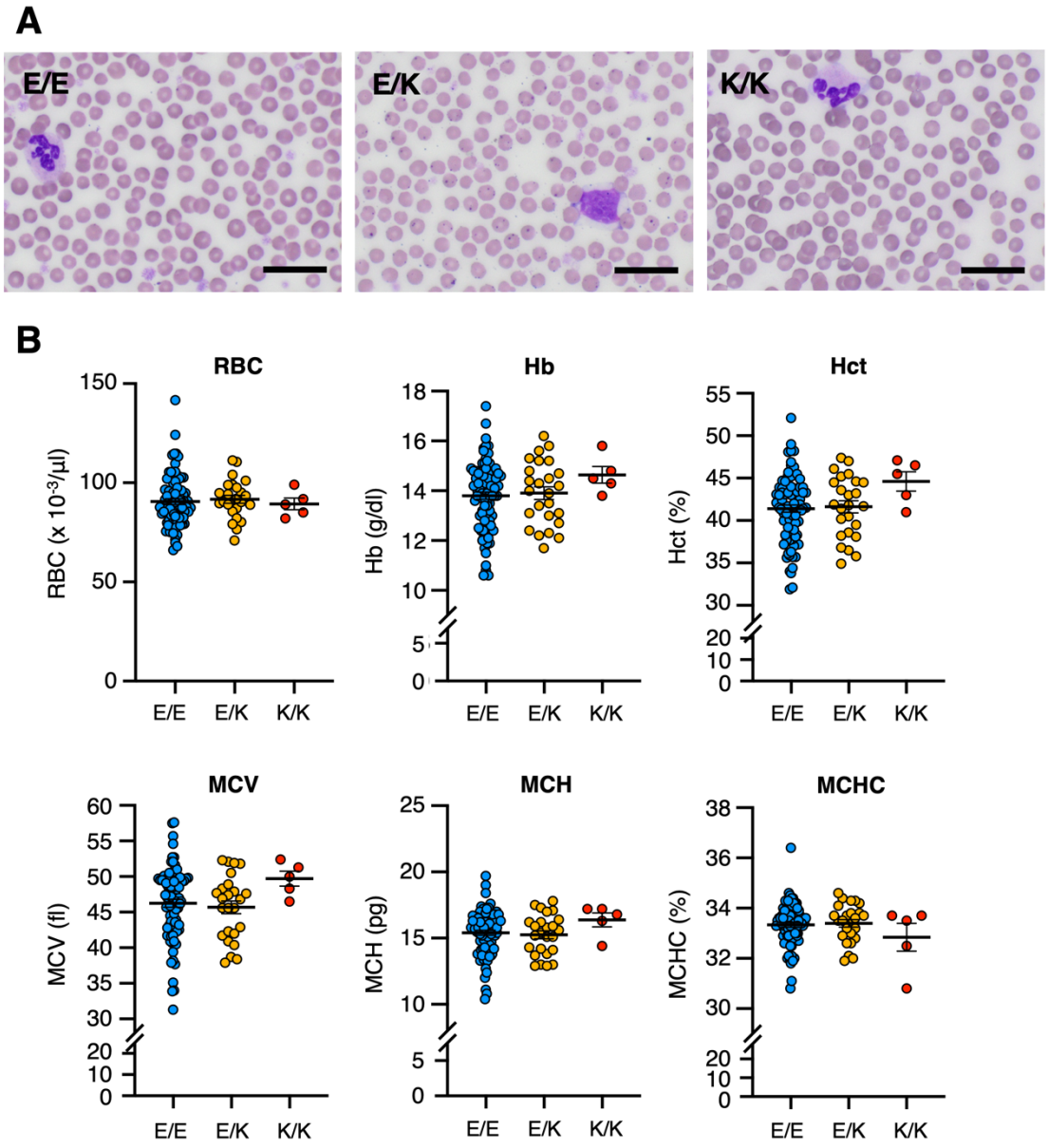

Figure 5. Morphology and hematologic parameters of cattle with different *SPTA1* genotypes. (A) The peripheral blood smears (Wright–Giemsa stain) from animals with different genotypes for E91K substitution (E/E, E/K, and K/K). Bars, 20 μm. (B) Hematologic indices including RBC counts (*RBC*), hemoglobin concentration (*Hb*), hematocrit values (*Hct*), mean corpuscular volume (*MCV*), mean corpuscular hemoglobin (*MCH*), and mean corpuscular hemoglobin concentration (*MCHC*) were examined for totally 114 animals with different *SPTA1* genotypes (*E/E*, n = 84; *E/K*, n = 25; *K/K*, n = 5). Data are expressed as the means ± S.E.M. No significant difference was observed for all indices among the genotypes by one-way ANOVA analysis with Tukey's multiple comparison test.